Gondwana Research 86 (2020) 126–143

Contents lists available at ScienceDirect

Gondwana Research

journal homepage: www.elsevier.com/locate/gr

GR Focus Review

Global Cenozoic Paleobathymetry with a focus on the Northern Hemisphere Oceanic Gateways

E.O. Straume [a,*], C. Gaina [a], S. Medvedev [a], K.H. Nisancioglu [a,b,c]

[a] Centre for Earth Evolution and Dynamics, Department of Geosciences, University of Oslo, Norway
[b] Department of Earth Science, University of Bergen, Bergen, Norway
[c] Bjerknes Centre for Climate Research, University of Bergen, Norway

ARTICLE INFO

Article history:
Received 31 January 2020
Received in revised form 12 May 2020
Accepted 17 May 2020
Available online 25 June 2020

Handling Editor: M. Santosh

Keywords:
Oceanic Gateways
Paleobathymetry
Paleotopography
Marine geophysics
Plate tectonics
Ocean circulation

ABSTRACT

The evolution of the Northern Hemisphere oceanic gateways has facilitated ocean circulation changes and may have influenced climatic variations in the Cenozoic time (66 Ma–0 Ma). However, the timing of these oceanic gateway events is poorly constrained and is often neglected in global paleobathymetric reconstructions. We have therefore re-evaluated the evolution of the Northern hemisphere oceanic gateways (i.e. the Fram Strait, Greenland–Scotland Ridge, the Central American Seaway, and the Tethys Seaway) and embedded their tectonic histories in a new global paleobathymetry and topography model for the Cenozoic time. Our new paleobathymetry model incorporates Northeast Atlantic paleobathymetric variations due to Iceland mantle plume activity, updated regional plate kinematics, and models for the oceanic lithospheric age, sediment thickness, and reconstructed oceanic plateaus and microcontinents. We also provide a global paleotopography model based on new and previously published regional models. In particular, the new model documents important bathymetric changes in the Northeast Atlantic and in the Tethys Seaway near the Eocene–Oligocene transition (~34 Ma), the time of the first glaciations of Antarctica, believed to be triggered by the opening of the Southern Ocean gateways (i.e. the Drake Passage and the Tasman Gateway) and subsequent Antarctic Circumpolar Current initiation. Our new model can be used to test whether the Northern Hemisphere gateways could have also played an important role modulating ocean circulation and climate at that time. In addition, we provide a set of realistic global bathymetric and topographic reconstructions for the Cenozoic time at one million-year interval for further use in paleo-ocean circulation and climate models.

Contents

* Corresponding author.
E-mail address: e.o.straume@geo.uio.no (E.O. Straume).

https://doi.org/10.1016/j.gr.2020.05.011
1342-937X/

1. Introduction

Plate tectonics, mantle processes, and volcanism together with weathering, erosion, and sediment deposition shape the continuously changing morphology of the Earth's surface. Bathymetric and topographic changes driven by these processes influence ocean circulation and climate on geological timescales. In the Cenozoic (66 Ma–0 Ma), opening and closing strategic oceanic gateways located in both the Northern and Southern Hemisphere have facilitated major ocean circulation changes, which have played an important role in the transition from a greenhouse to an icehouse climate (e.g. Kennett, 1977; Sijp et al., 2014; Zachos et al., 2001; Zhang et al., 2011). In the literature so far, much attention has been given to the oceanic gateways in the Southern Hemisphere, the Drake Passage and the Tasman Gateway, mainly because of their postulated contribution to the Antarctic glaciation that started at the time of the Eocene–Oligocene Transition (e.g. Eagles and Jokat, 2014; Kennett, 1977; Lawver and Gahagan, 2003; Livermore et al., 2005; Scher et al., 2015; Stickley et al., 2004). The opening of Southern Ocean through the Tasman Gateway and Drake Passage eventually enabled the flow of the Antarctic Circumpolar Current (ACC) (e.g. Kennett, 1977; Scher and Martin, 2006; Scher et al., 2015; Sijp et al., 2011; Toggweiler and Samuels, 1995), which presumably created the right conditions for the growth of the first Antarctic ice sheets close to the Eocene–Oligocene Transition - a turning point in the complex Cenozoic cooling trend (e.g. Kennett, 1977; Stickley et al., 2004; Zachos et al., 2001). The timing and role of southern oceanic gateways are still a matter of debate (e.g. Eagles and Jokat, 2014; Livermore et al., 2005; Scher and Martin, 2006; Scher et al., 2015; Stickley et al., 2004); besides, alternative mechanisms such as decreasing atmospheric CO_2 levels (e.g. DeConto and Pollard, 2003; Pagani et al., 2011) or other oceanic gateway events (e.g. Abelson and Erez, 2017; Zhang et al., 2011) have been proposed as triggers for this cooling.

The circulation in the world's oceans depends on both Southern and Northern Hemisphere oceanic basins and gateways, and our goal is to better document the Cenozoic tectonic evolution of the Northern Hemisphere oceanic gateways and contribute to a more detailed view of Cenozoic paleobathymetry. In the Northern Hemisphere two oceanic gateways closed (the Tethys Seaway and the Central American Seaway-CAS), and three gateways opened (the Greenland–Scotland Ridge-GSR, the Fram Strait and the Bering Strait) during Cenozoic. Previous studies provide a wide range of estimates to when these gateways opened or closed. For example, the range of estimates for the subsidence of the GSR (including the Faroe-Shetland Channel) spans almost 30 Myrs from the Mid Eocene to the Mid-Late Miocene (e.g. Clift and Turner, 1995; Davies et al., 2001; Denk et al., 2011; Hohbein et al., 2012; Poore et al., 2006; Wold, 1995); the time for the closure of the Tethys Seaway varies by ~30 Myrs from Early Eocene to Mid Miocene (e.g. Allen and Armstrong, 2008; Harzhauser et al., 2007; Oberhänsli, 1992; Rögl, 1999), and the CAS timing approximations spans ~20 Myrs from Early Miocene to Pleistocene (e.g. Duque-Caro, 1990; Marshall et al., 1982; Montes et al., 2015; Montes et al., 2012b; Webb, 2006). Narrowing the timing of these gateway events is important. For example, the deepening of the GSR and the Fram Strait provided the only deep-water connection to the Arctic Ocean, through the NE Atlantic, which was crucial in developing the modern Atlantic Meridional Overturning Circulation (AMOC) (Abelson and Erez, 2017; Jakobsson et al., 2007; Thiede and Myhre, 1996; Wright and Miller, 1996). Likewise, shallowing of the Tethys Seaway and the CAS would have increased the salinity differences between the Atlantic and Pacific Oceans, favoring a stronger AMOC (Maier-Reimer et al., 1990; Nisancioglu et al., 2003; Sepulchre et al., 2014; Zhang et al., 2011). Together with the changes in Southern Ocean gateway configurations, the opening and closing of the Atlantic-Arctic oceanic gateways (e.g. Coxall et al., 2018; Hutchinson et al., 2019), or shallowing of the Tethys Seaway (e.g. Allen and Armstrong, 2008; Zhang et al., 2011) could have played an important role in triggering the Eocene–Oligocene cooling by promoting deep water formation in the North Atlantic and a strengthening of the AMOC. From the Oligocene and throughout Miocene, pulsations in the Iceland mantle plume caused temporal uplift and subsidence of the GSR which is thought to have induced changes in the production of Northern Component Water (NCW) and thereby influenced global ocean circulation (Parnell-Turner et al., 2014; Poore et al., 2006; Wright and Miller, 1996). The shallowing of the Tethys Seaway, and the later uplift of the Panama Isthmus has also been linked to more recent climatic changes like the Mid Miocene climatic transition (Hamon et al., 2013; Nisancioglu et al., 2003) and the Northern Hemisphere glaciations (e.g. Haug et al., 2001; Lear et al., 2003).

The decreasing atmospheric CO_2 levels in the Cenozoic, alongside the tectonic changes in continent-ocean geometry and geography were probably essential to explain the observed climatic changes (Zachos et al., 2008). It is important to note that changes in atmospheric CO_2 could also be a consequence of tectonically driven changes in silicate weathering (e.g. Raymo et al., 1988), as for example, Himalayan orogeny related weathering (e.g. Allen and Armstrong, 2008; Raymo, 1994) or oceanic gateways associated shift in precipitation pattern and implicit alterations in weathering rates (Elsworth et al., 2017).

Given the importance of oceanic gateways for the climate evolution, our goal is to re-evaluate the tectonic evolution of the Northern Hemisphere oceanic gateways active in the Cenozoic (i.e. the Fram Strait, Greenland–Scotland Ridge, the Central American Seaway, and the Tethys Seaway) and construct novel or updated paleobathymetric models for these regions. These new models are then embedded in a new Cenozoic global paleobathymetry/topography model. Our model is based on improved plate kinematics and incorporates new constraints on sediment thickness, crustal thickness, continent-ocean transition, and a combination of new and previously published regional and global paleotopography models. We have evaluated our oceanic gateway model using geological evidence and paleo-oceanographic data from the literature, and in specific cases we made adjustments to provide the most realistic paleobathymetry for these gateways. Our aim is to provide a set of publicly available realistic reconstructions that can be implemented in paleo-ocean circulation and climate models.

2. Towards a new global paleobathymetry model

Paleobathymetry is one of the most important boundary conditions in paleo-ocean circulation models. The geometry of the oceanic basins determines the pattern of large-scale ocean circulation, mid-ocean ridges govern the amount of mixing in the oceans, and together with oceanic plateaus, they steer and deflects ocean currents (e.g. Polzin et al., 1997; Rebesco et al., 2014). Furthermore, the morphology of continental slopes influences the flow along the boundaries of the oceanic basins (e.g. Holland, 1973). To model paleobathymetry back in time we need information on plate tectonic kinematics and the evolution of oceanic lithospheric age (I), oceanic plateaus (II) and sediment thickness (III). We also need to know about the geometry and evolution of continental margins (IV) and sea level changes through time (V). We have therefore adopted a method for reconstructing the paleobathymetry that follows these five steps (Fig. 1):

(I) Oceanic lithospheric age and thermal subsidence

Oceanic basins subside as they grow older due to thermal subsidence. It follows that oceanic depth evolution through time can be directly inferred from oceanic lithosphere age, which in turn, is derived from its geophysical signature (mainly magnetic anomalies). For this study, we start with a global kinematic model that compiled a wealth of information about oceanic basin age and geometry evolution. The Straume et al. (2019) global model, is an update of the global kinematic model of Seton et al. (2012), including newer regional plate tectonic models of the African plate, Indian Ocean, NE Atlantic and the Arctic (Gaina et al., 2013, 2015, 2017, and Nikishin

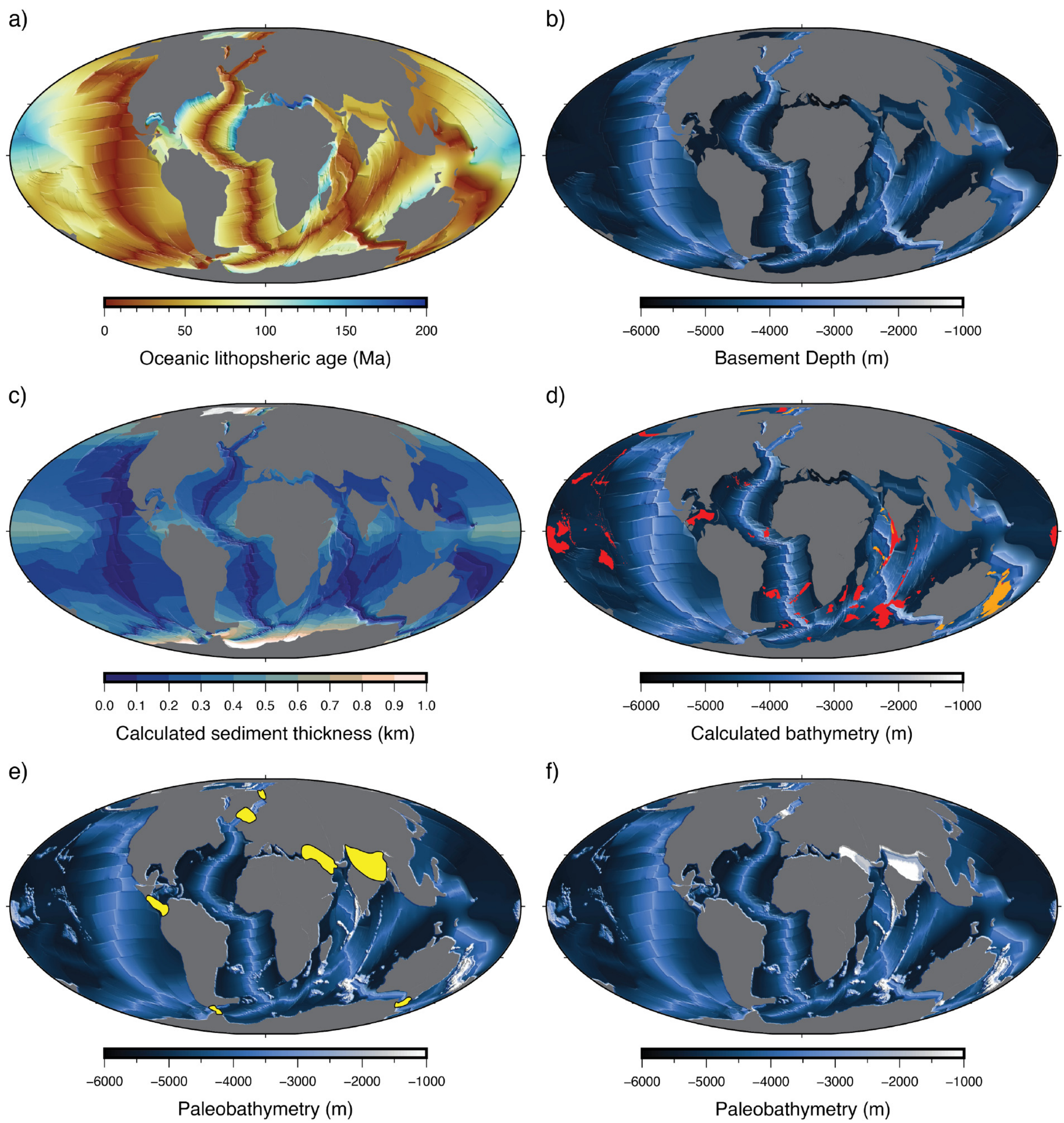

Fig. 1. Input models for calculating global paleobathymetry for a selected time near the Eocene–Oligocene boundary (34 Ma). a) Oceanic lithospheric age. b) Calculated basement depth. c) Calculated sediment thickness using the formula of Straume et al. (2019). d) Calculated bathymetry including sediment thickness, corrected for sediment loading. Red filled regions mark Large Igneous Provinces. Orange filled areas mark microcontinents. e) Paleobathymetry with reconstructed LIPs and microcontinents. Yellow filled regions mark areas where we applied corrections to the model accounting for details of key oceanic gateways. f) Paleobathymetry including adjustments to oceanic gateways.

et al., 2017, respectively), and the global Eocene reconstructions by Gaina and Jakob (2018). This improved global model was used to calculate oceanic lithospheric age for the Cenozoic and to compute the associated oceanic basement depth according to thermal subsidence for normal oceanic crust using the formulas of Crosby and McKenzie (2009):

$$d = \begin{cases} -2652 - 324\sqrt{\tau} & \tau \leq 75\,\mathrm{Ma} \\ -5028 - 5.26\tau + 250\sin\left(\dfrac{\tau - 75}{30}\right) & 75\ \mathrm{Ma b}\tau \leq 160\ \mathrm{Ma} \\ -5750 & \tau \mathrm{N} 160\ \mathrm{Ma} \end{cases}, \quad (1)$$

where d is the depth to basement, and τ is the age of the oceanic lithosphere in million years. This formula is not valid for regions of anomalous thermal subsidence (like oceanic plateaus, microcontinents, and large seamounts).

(II) Residual Bathymetry

In case of additional volcanic emplacement on oceanic floor, the simple bathymetry calculated in the first step has to be amended. Therefore, in the second step, we estimate the residual bathymetry of oceanic plateaus and microcontinents for correcting the paleo-depth. We apply the new method of Straume et al. (2019) where the present-day residual bathymetry of the anomalous regions is added to the bathymetry predicted from normal thermal subsidence. This is done for times younger than the age of volcanic emplacement of the oceanic plateaus. For their location, extent and age of volcanic emplacement, we use a modified version of the Cocks and Torsvik (2016) model for Large Igneous Provinces (LIPs).

(III) Sediment thickness

We calculate the predicted sediment thickness on the oceanic lithosphere using the global formula of Straume et al. (2019) derived from the statistical analysis of modern distribution of sediments:

$$Z(\lambda, \tau) = \sqrt{\tau}\left(52 - 2.46\lambda + 0.045\lambda^2\right) \tag{2}$$

were Z being sediment thickness in meters and λ is the absolute value of latitude in degrees. Eq. (2) is derived from the newly compiled oceanic lithospheric age grid and the new National Geophysical Data Center's (NGDC) total sediment thickness grid 'GlobSed' (Straume et al., 2019). We add the calculated sediment thickness to the calculated basement depth and account for the sediment loading using the isostatic correction method of Sykes (1996). Eq. (2) is an improvement compared to previously published sediment thickness models (e.g. Conrad, 2013; Goswami et al., 2015; Olson et al., 2016), as it was derived from the most recent global sediment thickness grid, and it accounts for strong latitudinal variations of sediment thickness observable in individual oceans as well as globally (Straume et al., 2019). See supplementary material (-Section S2) for comparison of calculated and gridded data with observations from selected drill sites.

Eq. (2) integrates sedimentation of the ocean floor from its formation to the modern time. The integration thus assumes that the average rate of sediment accumulation is proportional to $t^{-0.5}$, where t is the time measured in million years back. That time-dependent rate captures the substantial late-Cenozoic increase of sedimentation (Molnar, 2004) and general trend of sedimentation rate increase during last 80–85 Ma which may be expressed by the same functional dependence as in Eq. (2) (e.g. Olson et al., 2016). In our model, we reasonably assume that Eq. (2) is valid for the entire Cenozoic time and that the time dependence of the global sedimentation rate remains inversely proportional to square root of time from modern (~$t^{-0.5}$). The sediment thickness of τ My old oceanic crust t Ma is then:

$$Z(\lambda, \tau, t) = \left(\sqrt{\tau} - \sqrt{t}\right)\left(52 - 2.46\lambda + 0.045\lambda^2\right) \tag{3}$$

A comparison between modelled total sediment thickness using the above-mentioned formula and observed data from selected drill sites is presented in the supplementary material. Accounting for sedimentation using Eq. (3) has been shown to improve sea level reconstructions for the Phanerozoic, compared to reconstructions of basement depth solely calculated using Eq. (1) (Karlsen et al., 2020).

For completing the calculation of reconstructed oceanic basement depth through time, we add the calculated sediment thickness to the calculated basement depth and account for the sediment loading using the isostatic correction method of Sykes (1996).

(IV) Continental margins

Eqs. (2) and (3) were derived for deep ocean areas, considered to be at least 200 km away from the continent-ocean boundary (COB) and therefore not influenced in a considerable way by the continentally derived sedimentation. Oceanic gateways could be narrow passages close to continental margins, therefore a global analysis of paleobathymetry, especially with emphasis on oceanic gateways, however, also requires reconstructions of the areas adjacent to the COBs. The data on accumulation history of sediments in these regions is of various resolution, in most cases it lacks the accuracy needed to truthfully restore the amount of sediments accumulated at certain relevant time intervals. Dutkiewicz et al. (2017) presented a complex regression algorithm, which works well close to continental margins by accounting for the age, distance to continents, and proximity to major rivers. Here, we derive a new regression for sediments along continental margins aiming for simplicity and compatibility with Eq. (2). The main assumption of our simplified approach is that the sediments thickness along margins has the same functional dependence on age and latitude as in the Eqs. (2) and (3):

$$Z_m(\lambda, \tau_m) = \left[k\sqrt{\tau_m} + A_0\right]\left(52 - 2.46\lambda + 0.045\lambda^2\right) \tag{4}$$

The two terms in square brackets present two phases of sediment evolution: pre-breakup (syn-rift) sediments are quantified by parameter A_0, whereas post-breakup sediments are described by τ_m, the age of breakup in My (approximated by the nearest ocean floor age), and coefficient k. We estimate parameters $A_0 = 17$ and $k = 2.2$ by optimizing Eq. (4) using data from GlobSed (Straume et al., 2019). The resulting regression as well as any other globally derived relations, has limited predictive power for a specific margin because of great variations of sediments worldwide for the same age and latitude, but Eq. (4) presents a normal/non-eventful evolution of sediments along the margins. The equation predicts the equivalence of pre- and post-breakup sediment thickness ca. 60 My after breakup, which corresponds well to analytical solutions (Hartz et al., 2017). The comparison of Eqs. (3) and (4) shows a naturally faster ($k = 2.2$ times) post-breakup sediments accumulation near continental margins supported by stronger influx of eroded materials from continents.

For the continental margins, we reverse the process outlined above (III), by taking today's global sediment thickness grid (i.e. GlobSed) and remove sediments younger than the age of reconstruction and account for the subsidence of the margins related to sediment loading. According to Eq. (4), the amount of sediments to remove from the continental margin to reconstruct their thickness at time t Ma is:

$$\Delta Z_m(\lambda, \tau_m, t) = 2.2\left(\sqrt{\tau_m} - \sqrt{\tau_m - t}\right)\left(52 - 2.46\lambda + 0.045\lambda^2\right) \tag{5}$$

We define the transition zone between continental and oceanic lithosphere as the region within 75 km from the COBs (in our model, the COBs modified from Cocks and Torsvik (2016)). By assigning a transitional region from continent to ocean we are able to also account for the continental rise, which is characterized by landward shallowing of the oceanic lithosphere in the vicinity of the COB (e.g. Goswami et al., 2015). Within this area, we extract bathymetric contour lines per 100 m intervals, then we smooth them, make a grid and blended it at the edges using the GMT routines 'surface' and 'grdblend' (Wessel et al., 2013). Bathymetry and sediment thickness in the transition zone is computed by linking solutions from (III) and (IV).

(V) Sea level fluctuations

Paleobathymetric reconstructions need to consider the eustatic sea-level variations. There are many different sea level curves published so far (see Karlsen et al. (2019) or Müller et al. (2008) and references therein for detailed reviews), and depending on selection, the resulting paleobathymetry may change on the order of ~100 m, and the differences are greater the further you go back in time (Müller et al., 2008). We account for the sea level changes using the global curve of Haq and Al-Qahtani (2005) which has smooth and more realistic sea-level variations, in contrast to rather low values of (e.g. Miller et al., 2005) or too high as in (e.g. Xu et al., 2006) (see Müller et al. (2008) for details).

3. Detailed reconstructions of the Northern Hemisphere oceanic gateways

We aim to document the Cenozoic evolution of key Northern Hemisphere oceanic gateways and provide a global paleobathymetry model that includes detailed reconstructions of these gateways. In order to better follow the evolution of the selected oceanic gateways (i.e. the Fram Strait, Greenland–Scotland Ridge, the Tethys Seaway, and the Central

American Seaway) according to available literature and argue for our preferred model, the following subsections are structured as following: We start with an introduction presenting the background review of the selected gateway, followed by a description of the existent local tectonic models (also succinctly presented in Tables 1–4), and finally we present adjustments applied to the respective gateway model in order to achieve a more realistic and detailed representation of the gateway region at relevant times. Therefore, the detailed models presented in this section aim to improve the global models obtained by applying the methodology described in Section 2. Reconstructing the detailed spatial evolution of gateway regions is crucial for better understanding the role of tectonics in climate changes.

3.1. The Atlantic-Arctic oceanic gateways

3.1.1. The Fram Strait

The Fram Strait is the only deep-water gateway to the Arctic Ocean. The opening of the Fram Strait enabled deep-water exchange between the northern North Atlantic and the Arctic Ocean. This was paramount for the circulation regime in the Arctic Ocean, and could have been important for global ocean circulation and climate by influencing the production of North Atlantic Deep Water (NADW) and initiating the Atlantic Meridional Overturning Circulation (AMOC) (e.g. Hutchinson et al., 2019; Jakobsson et al., 2007; Knies and Gaina, 2008). During the Miocene, the Arctic Ocean changed from a poorly oxygenated isolated ocean, to a fully ventilated ocean, which was most likely a result of widening and deepening of the Fram Strait (Jakobsson et al., 2007). It has been suggested that the Fram Strait started to open already in the Early Oligocene (around magnetic anomaly Chron 13) (Engen et al., 2008), although it probably remained quite shallow until the Miocene because it may have not subsided sufficiently, was blocked by terrigenous sediments, or the Hovgård microcontinent (now submerged) acted like a barrier until Miocene times (Engen et al., 2008; Kaminski et al., 2005; Myhre et al., 1995a; Thiede and Myhre, 1996). The suggested timing for the Fram Strait opening is in the Early to Mid-Miocene (see Table 1). Note that the timing from studies based on geophysical data and plate kinematics (e.g. Engen et al., 2008; Jokat et al., 2016) converge towards an earlier opening time than suggested by paleo-oceanographic studies which are based on sedimentation and microfossils age (Jakobsson et al., 2007; Myhre et al., 1995b). This discrepancy may indicate that even though oceanic crust formed in the gateway, the depth was shallower than predicted by general thermal subsidence formulas (e.g. Crosby et al., 2006; Crosby and McKenzie, 2009; Stein and Stein, 1992), possibly for the reasons stated above.

It is therefore imperative to also consider the role of oceanic plateaus and microcontinents that may have restricted the flow through the gateway (Knies and Gaina, 2008; Knies et al., 2014) when reconstructing the Fram Strait paleobathymetry. Here, we calculate and add the residual bathymetry for the Yermak Plateau, Greenland Ridge, and the Hovgård microcontinent (HMC) to their reconstructed locations through time. However, the resulted paleobathymetry of the HMC is still deeper than expected from geological evidence (e.g. Knies et al., 2014; Matthiessen et al., 2009; Myhre et al., 1995b). The HMC was probably subaerial from ~25 Ma to 6.7 Ma, and may have restricted deep water exchange through the Fram Strait until the Early Pliocene (Knies et al., 2014). To account for a subaerial HMC in that period, the residual bathymetry of the microcontinent had to be ~50% shallower than today, so we increased the residual bathymetry of the HMC by 50% for times older than 8 Ma, and gradually reduce the added magnitude to its modelled value by 5 Ma.

Table 1
Evidence of Fram Strait structure and evolution.

Timing	Depth	Proxy	Reference
20–15 Ma	Narrow oceanic corridor, depth uncertain	Bouguer gravity map, integrated with seismic data	Engen et al. (2008)
Middle Miocene	~2 km	Tectonic model and (poorly known) depositional environment between Svalbard and Greenland	Kristoffersen (1990)
Middle Miocene	2.5 km–2.8 km	Plate kinematics and paleobathymetry model	Knies and Gaina (2008)
20–17 Ma (partly open), 11.2 Ma (open)	Shallow/narrow, deep at 11,2 Ma	Changes in sedimentation regime from ODP Site 909	Myhre et al. (1995b)
17.5 Ma (partly open) 13.7 Ma (open)	>2 km by 13.7 Ma	Arctic Ocean sediment cores, IODP expedition 302	Jakobsson et al. (2007)
21 Ma	Possible shallow seaway before 21 Ma, deepens afterwards	Geophysical evidence, aeromagnetic surveys	Jokat et al. (2016)
17 Ma	>1.5 km	Geological and geophysical data	Ehlers and Jokat (2013)

Table 2
Evidence of a submerged Greenland–Scotland Ridge, modified from Denk et al. (2011).

Greenland–Iceland Ridge	Iceland–Faroe Ridge	Faroe–Shetland Channel	Proxy	Reference
Oligocene/Miocene	Oligocene/Miocene	Early Eocene	Vertebrates	McKenna (1983a, 1983b).
~35 Ma	25–30 Ma	30–35 Ma	Model based on geological and geophysical data	Wold (1995)
15–18 Ma	15–18 Ma	Early Cenozoic	Model and geological evidence	Poore et al. (2006)
15–18 Ma	Mid–Miocene	40–50 Ma	Geological evidence	Thiede and Eldholm (1983)
18–13 Ma	18–13 Ma	18–13 Ma	Benthic foraminifera	Ramsay et al. (1998)
6 Ma	10 Ma	10 Ma	Paleontological evidence (plant fossils)	Denk et al. (2011)
Oligocene/Miocene	Oligocene/Miocene	–	Geological and paleontological evidence	Talwani et al. (1976), Berggren and Schnitker (1983). Interpreted by Ellis and Stoker (2014)
–	–	49–50 Ma	Contourite drift	Hohbein et al. (2012)
–	–	~35 Ma	Contourite drift	Davies et al. (2001)

3.1.2. The Greenland–Scotland Ridge

The Nordic Seas (i.e. the Greenland, Iceland, Norwegian, and Barents Seas) play a very important role in deep-water formation. The deep water formed in the Nordic Seas flows southward crossing the Greenland–Scotland Ridge (GSR) into the North Atlantic, where the dense overflow constitutes a considerable part of the North Atlantic Deep Water (NADW) (e.g. Mauritzen, 1996). Today, the NADW accounts for about half of the global production of deep water (Broecker et al., 1998). The amount of deep water exiting the Nordic Seas is controlled by the depth of the GSR, which has been deepening during the Cenozoic. However, the subsidence history of the GSR is not fully understood, and there are large differences in the estimations as to when the different parts of the ridge subsided (see Table 2). The role of its paleobathymetry in the transition from greenhouse to icehouse climate in the Cenozoic time is uncertain and its former depths are often undervalued in previous global paleobathymetric reconstructions (e.g. Bice and Marotzke, 2002; Herold et al., 2014; Herold et al., 2008; Zhang et al., 2011).

The GSR can be divided into three main segments; the Greenland–Iceland Ridge, the Iceland–Faroe Ridge, and the Faroe–Scotland Ridge which includes the Faroe–Shetland Channel (FSC) (Table 2, and Fig. 2). According to Beard (2008), all three segments were probably subaerial in the Early Eocene (~47 Ma), making the GSR a continuous land bridge. This was based on the discovery of *Tieilhardina magnoliana*, a mammal fossil found in Eocene deposits in Belgium, which presumably had migrated from North America to Europe over the North Atlantic Land Bridge (NALB) (Beard, 2008). In Table 2, we have summarized the span of estimates of when the GSR different sections subsided below sea level. They are quite different and make the timing of opening rather unconstrained. It is also a fact that after the continental break-up between Greenland and Eurasia (~55 Ma), the subsidence of the GSR has been influenced by the Iceland mantle plume. During that time, the variations in plume activity, as recorded by V-shaped ridges straddling the Reykjanes Ridge, have modulated the depth of the GSR (e.g. Jones et al., 2002; Parnell-Turner et al., 2014; Wright and Miller, 1996). Episodes of uplift and subsidence caused by variations in plume activity, could have opened and closed the oceanic gateway several times during the Cenozoic. This opens the possibility that more than one of the estimates of an open gateway in Table 2, could be correct.

Today, the depths of the NE Atlantic Ocean and the Greenland–Scotland ridge are anomalously shallow with respect to predicted normal thermal subsidence of the oceanic lithosphere. There are two main factors that cause the anomaly, and both must be accounted for in our paleobathymetric reconstructions of the NE Atlantic Ocean. First, the Greenland–Iceland–Faroe Ridge (GIFR) is isostatically supported by anomalously thick oceanic crust. The crustal thickness varies between 17 and 35 km, with values above 40 km beneath Iceland (Funck et al., 2017). This is ~2–5 times thicker than the 7 km thick normal oceanic crust (White et al., 1992). Second, the Iceland mantle plume dynamically supports the Greenland–Scotland ridge which contributes significantly to the shallow bathymetry (e.g. Jones et al., 2014).

3.1.2.1. Corrections for anomalous crustal thickness. We use the NE Atlantic crustal thickness grid of Funck et al. (2017) to calculate the isostatic effect of increased crustal thickness along the GIFR (see Supplementary figure, S3–S7). The resulting values were used to adjust our bathymetry calculated assuming normal thermal subsidence of the oceanic crust. For every time step, we use our plate kinematic model to rotate the crustal thickness to its paleo-location and remove crust younger than the age of reconstruction at the Mid-Atlantic ridge. The isostatic effect of crustal thickness is then added to bathymetry from calculated thermal subsidence and sedimentation. The crustal thickness is anomalously high along strike of the GIFR which has oceanic crustal ages spanning from 0 to 55 Ma (Straume et al., 2019). This implies that there have been high crustal thicknesses along the GIFR ever since continental break up (~55 Ma), and we therefore presume that the method of adding extra bathymetry based on crustal thickness is reliable. Our applied methodology is similar to previous models of the region (i.e. Ehlers and Jokat, 2013; Wold, 1995), however, we include more recent plate kinematics, lithospheric age, sediment thickness and crustal thickness data, and apply a new model for variations in dynamic support and locations of the Iceland plume (see below).

3.1.2.2. Corrections for mantle dynamic support. Today, the Iceland mantle plume dynamically supports region that covers a considerable part of the NE Atlantic Ocean, from continental Greenland to the NW European margin (Jones et al., 2014). Temperature pulsations in the Iceland plume have caused temporal uplift and subsidence on the ridge since continental break-up, and both short-term pulsations (with periodicity <10 Myrs), and long-term variations (>10 Myrs) in shape and size of the Iceland plume swell have occurred through time (Jones et al., 2002; Parnell-Turner et al., 2014; Poore et al., 2006; Wright and Miller, 1996). We approximate the dynamic topography caused by the Iceland Plume using a Gaussian shaped swell centred on Iceland. To determine the paleo-locations of the Iceland plume we use the hotspot track of Doubrovine et al. (2012), based on a global moving hotspot reference frame. The maximum dynamic topography values are varied according to the residual depth estimates of Parnell-Turner et al. (2014). We keep the FSC closed prior to ~36 Ma, and from 35 Ma the depths vary according to the influence from the plume and sedimentation (Fig. 2).

3.1.3. Uncertainties in NE Atlantic paleobathymetry reconstructions

Accounting for Iceland plume pulsations and long-term dynamic support variations introduces a new element of temporal vertical motions of the seafloor that captures more realistically the bathymetric evolution of the NE Atlantic Ocean and thereby significantly improving our model. However, there are uncertainties involved in this reconstruction method. For example, one would not expect that the plume swell is or has been symmetric (e.g., Jones and White, 2003), and the extent of the plume swell and the plume flux in the Cenozoic time is not easily constrained (e.g., White and McKenzie, 1989; Jones and White, 2003; Jones et al., 2014; Parnell-Turner et al., 2014). Also, there are many different predictions of the location of the Iceland Plume through time (e.g. Lawver and Müller, 1994; Jones and White, 2003; Doubrovine et al., 2012) depending on the global and regional plate kinematics and whether the mantle plume is considered fixed to the mantle (like in Lawver and Müller, 1994) or tilted by advection (like in Doubrovine et al., 2012).

The only manual adjustment we applied in the NE Atlantic region is to keep the FSC closed before 36 Ma. According to Hohbein et al. (2012), the onset of the "Judd Falls Drift", a proposed contourite drift deposit in the Faeroe-Shetland Basin, represents overflow of deep water from the Nordic Seas to the North Atlantic already at ~49 Ma. This interpretation indicates that the FSC was open at least two million years before *Tieilhardina magnoliana* supposedly crossed the North Atlantic Land Bridge. However, this assessment has been criticized by Stoker et al. (2013), arguing that their interpretation was flawed and that there are no real evidence of a deep-water connection before the synclinal form of the Faroe Bank Channel was created in the Miocene (Stoker et al., 2013; Stoker et al., 2005). We acknowledge that there are uncertainties in the opening of the FSC, however, we take the contourite drift supposedly deposited at ~35 Ma (see Section 3.1.2 and Davies et al. (2001)) to be the first indication of an open channel and implement this assumption into our final paleobathymetry model.

3.2. The Tethys Seaway

The Tethys Seaway connected the proto-Mediterranean Sea and the Indian Ocean. In the Early Cenozoic, the open Tethys Seaway along with the Central American Seaway (CAS) and the Indonesian Gateway provided a low latitude circum-global connection between the major world oceans. The shallowing of the Tethys Seaway has been shown to increase the salinity differences between the Atlantic and the Pacific Oceans and thereby increase the deep water formation in the North Atlantic

Table 3
Evidence and timing for closing the Tethys Seaway.

Timing	Depth	Proxy	Reference
10 Ma	Subaerial	Plate kinematics based on paleomagnetic data	Dercourt et al. (1986)
20 Ma	Subaerial	Apatite fission tracks	Okay et al. (2010)
19 Ma	Subaerial	Mammal exchange	Harzhauser et al. (2007)
28–23 Ma (restricted connection, where last possible closing is 11 Ma)	350 m–750 m (Early Oligocene). <350 m (Late Oligocene). 11 Ma closed.	Biostratigraphically dated Oligocene–Miocene sediments	Hüsing et al. (2009)
~34 Ma (Eastern Tethys)	Subaerial, however, this is only for the Eastern part, could still be an open seaway	Marine Paleogene sediments, Tibet	Wang et al. (2002)
~19 Ma	Subaerial, but temporal reopening of a shallow seaway at ~16 Ma	Model + marine sediments. Reopening is interpreted from Miocene marine sediments in the Lake Van area (Gelati, 1975)	Rögl (1999)
~35 Ma	Closed as a deep gateway, possibly subaerial	Structural geological evidence, (and sediments)	Allen and Armstrong (2008)
~16 Ma	Subaerial	Sedimentary evolution of the Qom formation	Reuter et al. (2009)
~49 Ma	End in export of warm saline bottom water to the Indian ocean, not an indication of final closure, but could indicate restricted flow and a shallow seaway	Sedimentary sequences, evaporate distribution	Oberhänsli (1992)

(Hamon et al., 2013; Zhang et al., 2011). Subsequently, this could have influenced the ocean circulation and climate in the Late Eocene/Early Oligocene time (Allen and Armstrong, 2008; Zhang et al., 2011), but also later in the Mid Miocene (Hamon et al., 2013; Ramsay et al., 1998). Both an Eocene/Oligocene and a Miocene shallowing of the seaway are supported by geological and oceanographic data (Allen and Armstrong, 2008; Oberhänsli, 1992; Okay et al., 2010; Rögl, 1999). The initial collision time between Arabia and Eurasia is not well constrained, but most studies postulate a time interval within the Eocene–Oligocene (~35–25 Ma) (e.g. Allen and Armstrong, 2008; Jolivet and Faccenna, 2000) to Early–Mid Miocene range (e.g. Okay et al., 2010; Robertson et al., 2007). There are indications of shallowing, and maybe even full closure of the Eastern Tethys in the Late Eocene (Allen and Armstrong, 2008). However, apatite fission track data from the Bitlis-Zagros thrust zone along with regional stratigraphy suggest that the last oceanic lithosphere between Arabia and Eurasia was consumed by ~20 Ma (Okay et al., 2010). This coincides with first animal migration over the "*Gomphotherium* Landbridge" at ~19 Ma (Harzhauser et al., 2007), and indicates the final closure of the seaway. After this time only shallow temporal connections between the Mediterranean and Indian Ocean were possible (e.g. Rögl, 1999). These connections may have existed until Mid–Late Miocene and isotope data suggests that warm saline waters possibly linked to the seaway was flowing into the northern Indian Ocean, and flowed south into the Southern Ocean (Hamon et al., 2013; Ramsay et al., 1998). The presence of this warm water in the Southern Ocean may have slowed the proto-ACC, therefore the closure of such a seaway could have been important for building the ACC strength and have contributed to the growth of the East Antarctic ice sheets during the Mid Miocene cooling event (Hamon et al., 2013; Woodruff and Savin, 1989; Wright et al., 1992).

Based on our initial kinematic global model, our modelled paleobathymetry results in a deep Tethys Seaway until ~10 Ma when our Arabian and Eurasian COBs (modified from Torsvik and Cocks (2016)) overlap. As the last oceanic lithosphere was consumed earlier than 10 Ma (around 20 Ma according ot Okay et al. (2010)) we re-evaluate the geometry of the northern Arabian block COBs considering a new kinematic model of the Mediterranean region (i.e. van Hinsbergen et al., 2019), and extend the COB to agree with the apatite fission track study of Okay et al. (2010). The Arabian COBs is extended to overlap with the Eurasian COBs at ~20 Ma to account for the lack of oceanic lithosphere at that time. We prescribe full closure of the seaway by ~19 Ma, which is also consistent with animal migration over the "*Gomphotherium* Landbridge" (Harzhauser et al., 2007). Before the seaway closure, our reconstruction method yields deep bathymetry (>4000 m) in the oceanic realm as the seaway was floored by old oceanic lithosphere. However, there are evidences of regional uplift in the Eocene (e.g. Allen and Armstrong, 2008) and shallower seaway depths in the Oligocene according to biostratigraphy (e.g. Hüsing et al., 2009). We therefore modify our model accordingly by assigning a shallower seaway (~2000 m–1000 m) from the Mid Eocene and onwards. The large discrepancy between the unadjusted model and observations is probably because the model does not capture all blocks and terranes that once existed in the seaway and uplift related to continent collision. The sill depth of which the Tethys close as an oceanic gateway with implications for regional and global ocean circulation is not known. Modelling suggests sill depths somewhere between 1000 m and 250 m (Hamon et al., 2013), which would correspond to an Early Oligocene to Early Miocene gateway closure according to our reconstructions (Fig. 3). However, we cannot rule out that the seaway may have stopped functioning as a deep ocean gateway already in the Eocene (Oberhänsli, 1992), or later in the Mid Miocene if any temporal continental straits were deep enough to matter (Hamon et al., 2013; Rögl, 1999).

3.3. The Central American Seaway

The Central American Seaway, CAS, located where the Panama Isthmus is today, was an oceanic gateway connecting the Pacific

Table 4
Evidence of Central American Seaway closure.

Timing	Proxy	Depth	Reference
3.1–2.7 Ma	Biotic exchanges between the Americas	Subaerial	Webb (2006)
~3 Ma	Interchange of land mammals between North and South America	Subaerial	Marshall et al. (1982)
12–7 Ma	Nd and Pb isotopes from fossil fish teeth and authigenic coatings of planktonic foraminifera	Closed for deep water exchange during this time. ~1000 m at 11.2 Ma	Osborne et al. (2014) & Newkirk and Martin (2009)
12.9–11.8 Ma	evaluation of Neogene stratigraphy and foraminiferal biostratigraphy	~1000 m	Duque-Caro (1990)
~15 Ma	Geochronological and geochemical data from the Isthmus of Panama	Subaerial (possible ~200 km wide and shallow opening in the Early Miocene)	Montes et al. (2012a) & Montes et al. (2012b)
15–13 Ma	Uranium-lead geochronology in detrital zircons, provenance analyses from boreholes, and stratigraphic sections in the Northern Andes	Closed, but Pacific–Atlantic water exchange could have taken place through transient, narrow, and shallow straits	Montes et al. (2015)

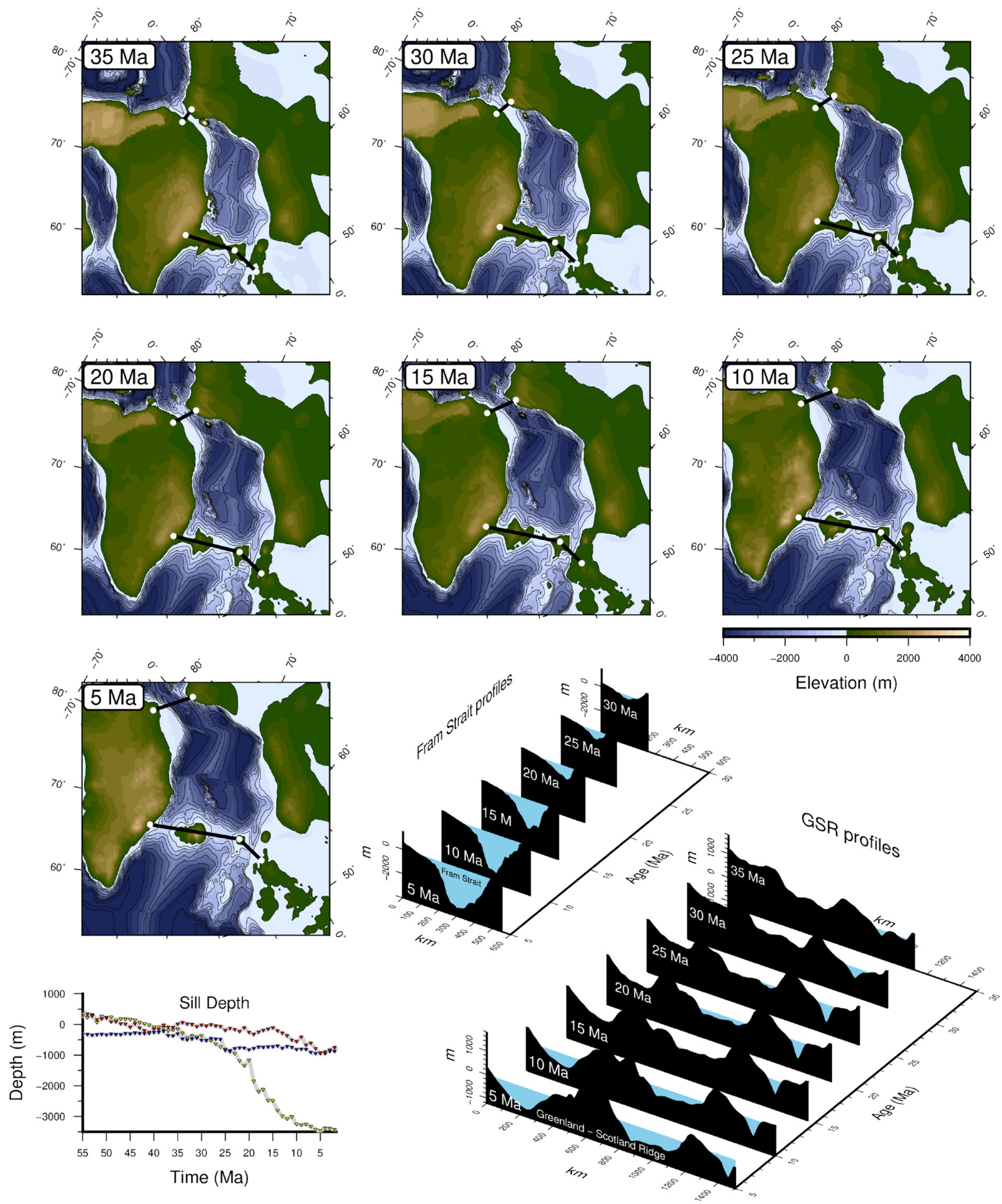

Fig. 2. Cenozoic paleobathymetry of the Atlantic–Arctic oceanic gateways and W-E profiles of the Fram Strait and Greenland–Scotland Ridge (GSR) showing their evolution from 35 Ma to 5 Ma. The sill depth reconstructions show the minimum elevation along the extracted profiles for every million-year since continental breakup between Greenland and Eurasia at 55 Ma. Sill depths for the Fram Strait = yellow, Greenland–Iceland–Faroe Ridge = red, and the Faroe–Shetland Channel = blue.

and Atlantic oceans (Fig. 4). Its closure is thought to have been important for the establishment of the modern day AMOC, as eastward flow through the gateway would reduce salinity in the Atlantic Ocean, and therefore limit the strength of the AMOC (e.g. Maier-Reimer et al., 1990; Sepulchre et al., 2014). Final closure of the gateway has been attributed to cause the American biotic interchange between North and South America at ~2.7 Ma (Marshall et al., 1982; Webb, 2006). Using this or a similar timing, several studies have proposed the closing of the gateway as an important factor for the initiation of the Northern Hemisphere glaciations (Haug et al., 2001; Lear et al., 2003). However, many authors suggest that the gateway shallowing occurred much earlier, several million years

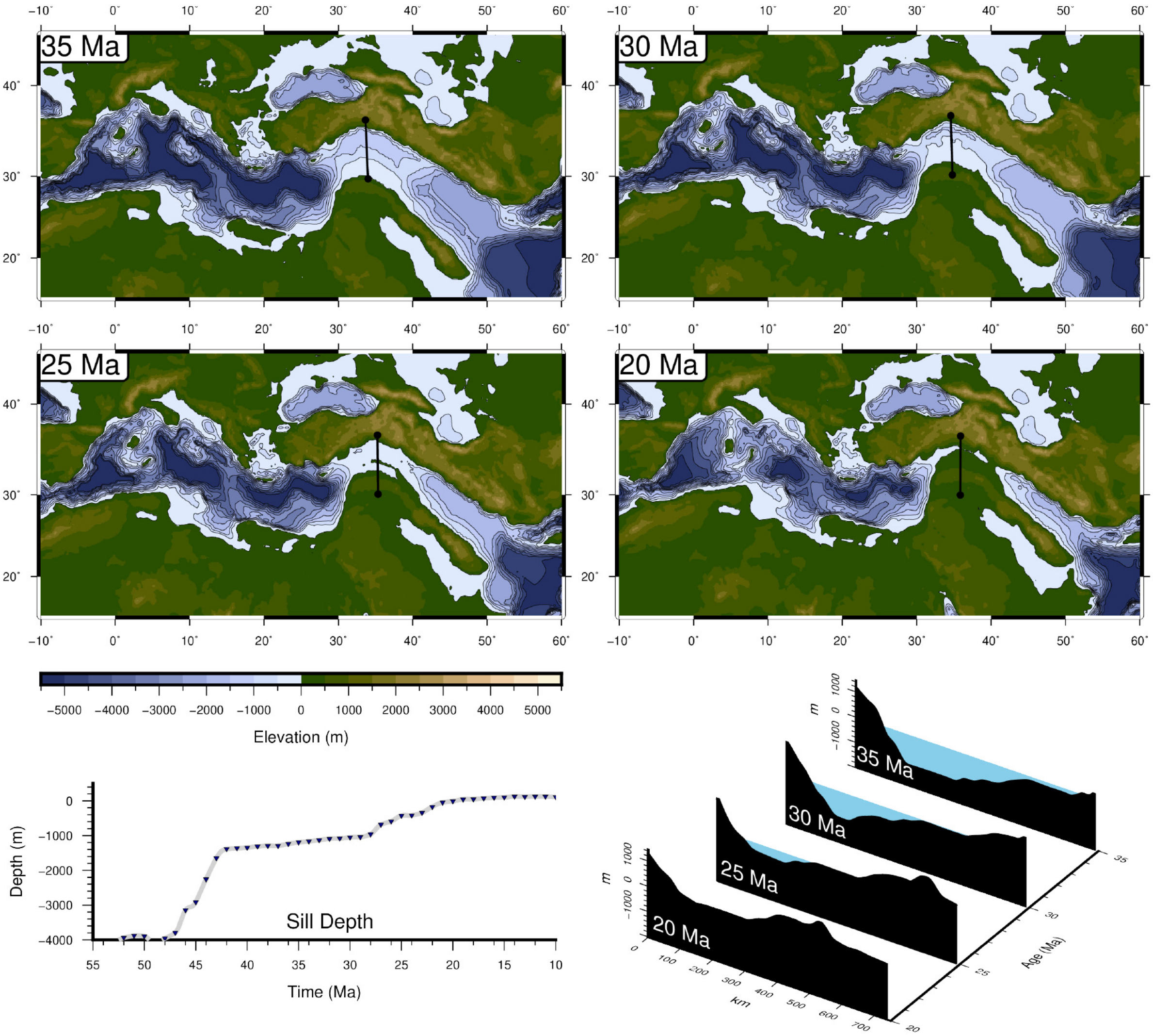

Fig. 3. Evolution of the Tethys Seaway with extracted N - S profiles. Sill depths represent the minimum elevation (deepest point) along the profiles for every millionth year from 55 Ma–10 Ma.

before full closure, and therefore the CAS was too shallow and narrow to significantly influence ocean circulation and climate in the Pliocene (Duque-Caro, 1990; Montes et al., 2012a; Montes et al., 2015; Montes et al., 2012b; Sepulchre et al., 2014). Evaluation of stratigraphy and foraminiferal biostratigraphy (Duque-Caro, 1990), and reconstructions of deep and intermediate water Nd and Pb isotope compositions from fossil fish teeth and planktonic foraminifera (Newkirk and Martin, 2009; Osborne et al., 2014), supports the hypothesis that the gateway shallowed to ~1000 m by Mid-Miocene times. The studies of Montes et al. (2012a, 2012b, 2015) go further in suggesting that there was only a shallow gateway, ~200 km wide near the Southern end of the Panama Isthmus, in the Early Miocene. Full closure occurred around 15–13 Ma, but transient shallow and narrow straits with some water exchange may have formed after that (see Table 4).

Following evidences documented by previous studies, we choose to keep an intermediate to shallow CAS (~2000 m) from the Late Eocene and prescribe further shallowing of the seaway in the Miocene as indicated above, leaving only narrow shallow straits by the Mid- Miocene. This favors the models of Montes et al. (2012a, 2012b, 2015). However, we do not implement a "forced" seaway closure before 3 Ma, taking into account that the American animal exchange around 2.7 Ma marked the full closure of the seaway (e.g. Marshall et al., 1982; Webb, 2006). A partly open seaway post Miocene time is also supported by evidence from planktonic foraminifera and Nd and Pb isotopes of fossil fish teeth indicating water exchange between the Atlantic and Pacific Oceans at that time (e.g. Newkirk and Martin, 2009; Osborne et al., 2014).

A Pliocene final CAS closure coincides in time with the opening of the Bering Strait and shallowing of the Indonesian Gateway (e.g. Karas et al., 2017; Marincovich and Gladenkov, 2001). In the present study we do not discuss at large these very recent gateway events; however, one should keep in mind that ocean circulation changes in the Pliocene could have also resulted from a combination of these gateway events.

As stipulated in the introductory statement, the geological history of the Southern Ocean gateways is amply discussed by many studies and a review of those gateways is beyond the scope of this paper. Our aim is to fill a gap in the literature and document in a comprehensive way the detailed evolution of the main Cenozoic oceanic gateways situated in the Northern Hemisphere. However, in order to have an updated global paleobathymetric model we have inspected the existing models for the Drake Passage and the Tasman Gateway and adopted models that respect a given set of first-order geological observations. A short description of these can be found in the Supplementary material.

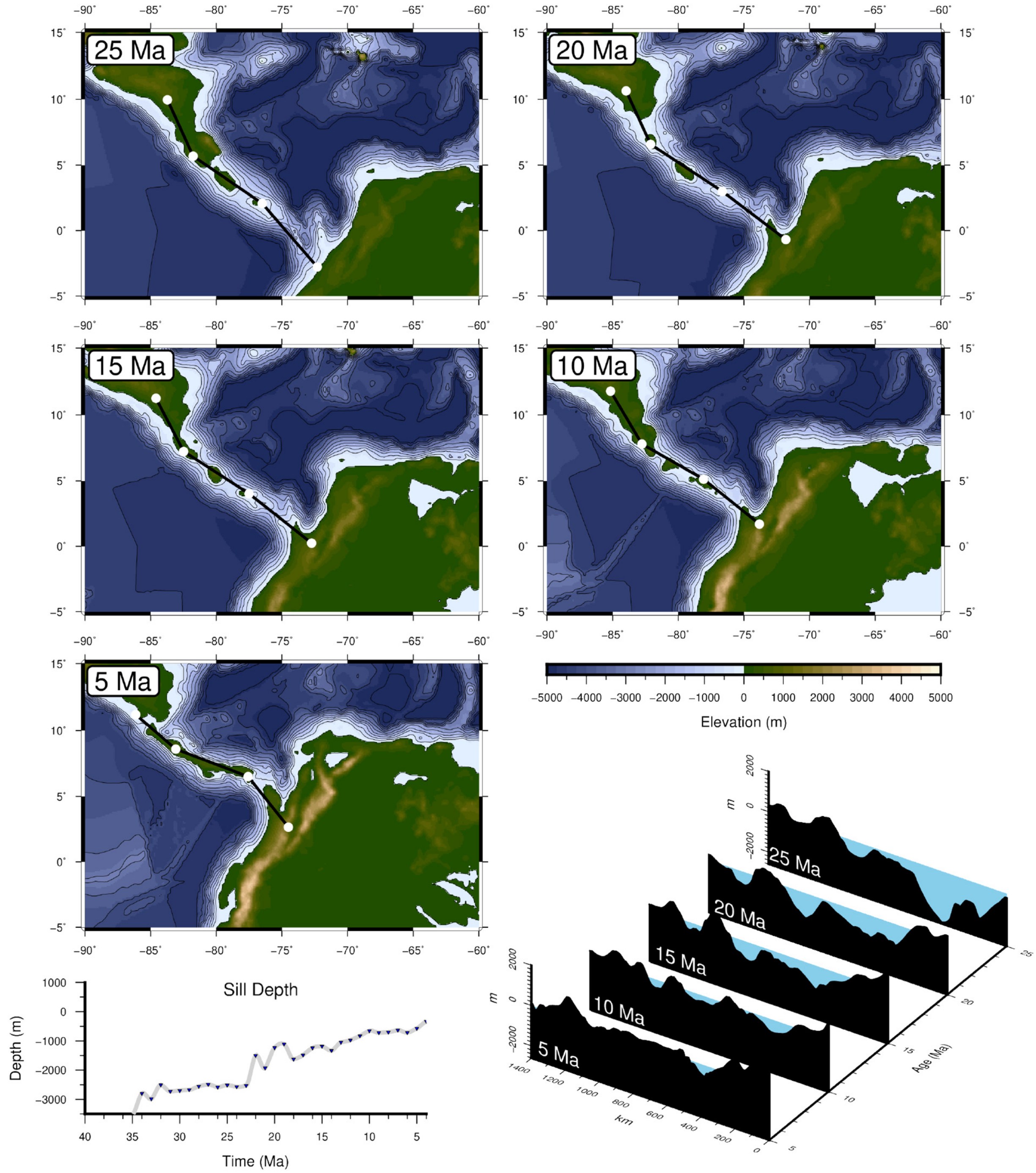

Fig. 4. Evolution of the Central American Seaway. NW–SW profiles extracted every 5 million year from 25 Ma–5 Ma. Sill depth is the minimum elevation along the profiles extracted with 1 million-year intervals.

4. Paleotopographic adjustments

Coupled climate models require complete models of topography and bathymetry. For increasing the usefulness of our global paleobathymetry model, we have prepared a global paleotopography model that accompanies the Cenozoic paleobathymetry model presented in this paper. The global paleotopography is a compilation of previously published and new regional models, and we use previously published global models (Cao et al., 2017; Herold et al., 2014; Herold et al., 2008) to compare, and in some cases adjust, our model.

For the circum-Arctic region, including Greenland and Scandinavia we adopt a new paleotopographic model based on the methodology of Medvedev et al. (2018), which calculates the pre-glacial topography of the circum-Arctic region by numerically restoring eroded material and calculating the flexural isostatic response. For the Mid–Late Miocene we combine this model with the regional model of Knies and Gaina (2008) for the Barents sea, based on the topography models of Rasmussen and Fjeldskaar (1996) and Dimakis et al. (1998). For the Eocene and Oligocene we add the new information from the paleoenvironment and erosion study of Lasabuda et al. (2018), which propose that the Barents Sea region was subaerial. In addition, we look at Cenozoic uplift and subsidence data from Anell et al. (2009) and adjusted our topography for the regions surrounding the North Atlantic through time.

For Antarctica, we use the newly published topographic reconstructions of Paxman et al. (2019). They reconstruct paleotopography of the

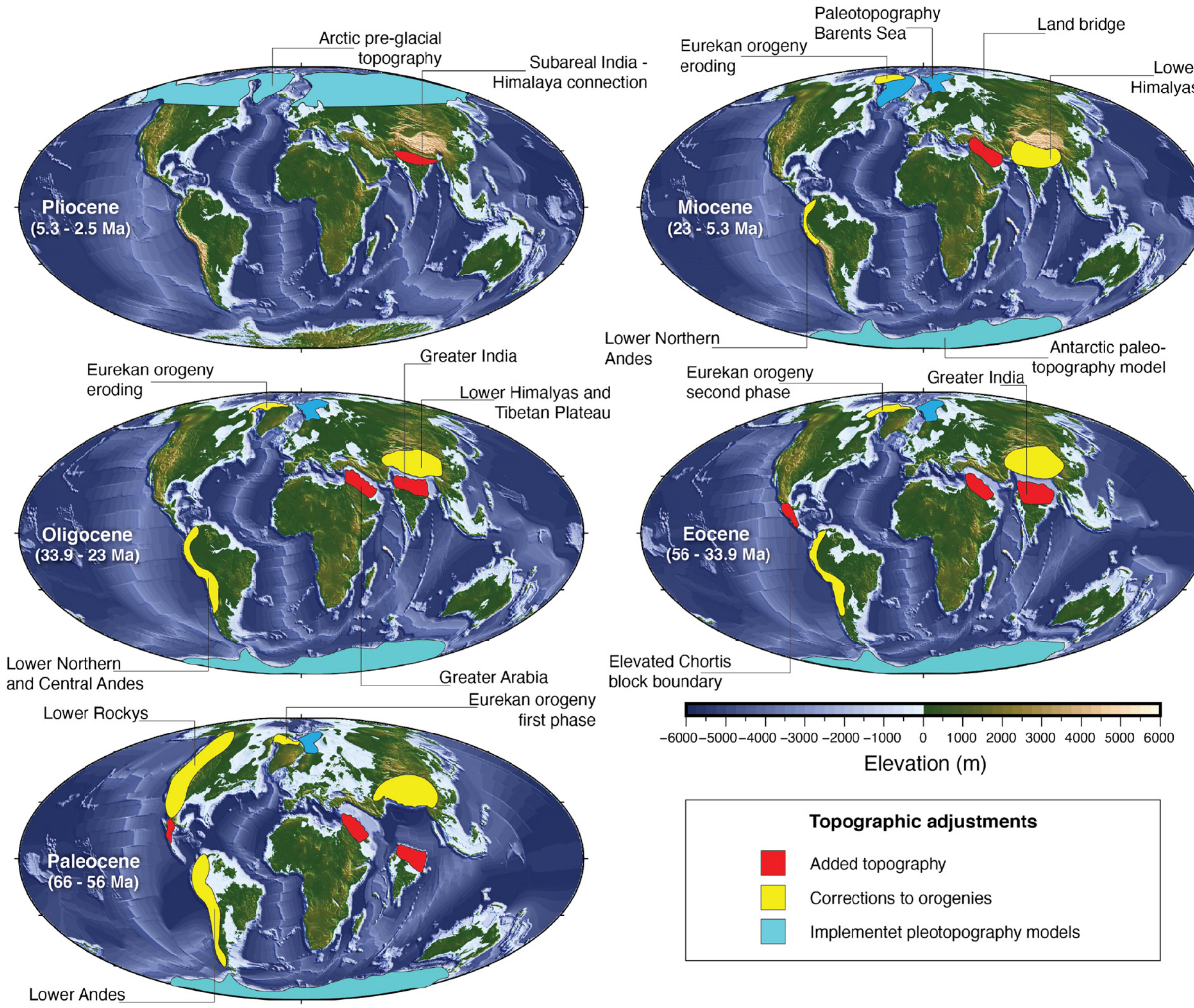

Fig. 5. Global paleotopography and regions of elevation adjustments. Colored regions indicate which regions were adjusted. Background reconstructions are 5 Ma for the Pliocene, 15 Ma for the Miocene, 25 Ma for the Oligocene, 36 Ma for the Eocene, and 56 Ma for the Paleocene.

Antarctic continent for four key time steps since the Eocene–Oligocene transition (i.e. 34 Ma, 23 Ma, 14 Ma and 3.5 Ma). This reconstruction does not go further back than 34 Ma, however, previous EOT reconstructions (i.e. ANTscape (Wilson et al., 2012)) has been applied for topographic reconstructions as far back as the Early Eocene (~55 Ma) (e.g. Herold et al., 2014). We use this configuration of Antarctica for the whole Eocene time. As there were no major ice sheets on Antarctica during this period, the topography changes were linked to other processes, mostly linked to tectonic events (Cramer et al., 2011; Herold et al., 2014). Due to the lack of useful paleotopographic models for times older than 34 Ma, we find the detailed and high-resolution model of Paxman et al. (2019) to be adequate for the Eocene time. For times younger than 34 Ma, we gradually change our model towards the 23 Ma paleotopography and repeat the process for the time interval 23 Ma to 14 Ma, and so on, until we reach the present-day topography. We use cosine-tapered weights to blend the topography between the modelled time steps using the Generic Mapping Tools command 'grdblend' (Wessel et al., 2013), where we change the weights at each time-step so we gradually go from one step to the next.

Other significant Cenozoic orogenic events that built the Himalayas, Andes, Rocky Mountains and the Eurekan were also incorporated in our global model. For the Himalayas and the Tibetan plateau, we keep a low relief, similar to Herold et al. (2014) for the Early Eocene. We gradually increase the elevation until the Middle Miocene when it is predicted that the Tibetan plateau reached modern day heights (e.g. Coleman and Hodges, 1995; Herold et al., 2008; Rowley and Currie, 2006; Williams et al., 2001).

Parts of the Andes Cordillera could have been at alpine heights in the Early Cenozoic, however, the mountain range was probably significantly lower than today (e.g. Markwick and Valdes, 2004). Periods of intensified Andean uplift have been recorded for the Early Eocene, Early Oligocene, Late Oligocene–Early Miocene, Mid Miocene and Early Pliocene (Hoorn et al., 2010). Previous topographic reconstructions have prescribed paleo-elevations in the central Andes to ~1000 m in the Late Cretaceous and Early Eocene (Herold et al., 2014; Markwick and Valdes, 2004), ~2000 m in the Late Eocene (Baatsen et al., 2016). Where the northern parts of the mountain chain did not reach high alpine elevation until Late Miocene times (Hoorn et al., 2010), we prescribe a low relief topography (~1000 m) in the Early Cenozoic, and gradually increase the central part until Late Miocene, where we assume a topography like the present day. We keep the northern part low (<1000 m) until Late Eocene, and increase the elevation to modern-day heights by Late Miocene after the model of Hoorn et al. (2010).

The North American Cordillera was probably high already in the Early Cenozoic (Abbey et al., 2017), and could have experienced ~4000 m by Mid-Eocene times (Chamberlain et al., 2012). We set a 50% lower relief in the Early Cenozoic and gradually increase the elevation until we reach modern day elevations at 35 Ma.

Compressional deformation, caused by simultaneous seafloor spreading in the Labrador Sea and NE Atlantic resulted in the Eurekan deformation and relief formation between NW Greenland and Ellesmere Island in the Eocene (Anell et al., 2009; De Paor et al., 1989). The maximum paleo-elevation of the orogeny is not certain. However, the recent study of Vamvaka et al. (2019) suggests a pronounced topographic growth during an exhumation period between ~44 Ma and 38 Ma. They suggest that the Eurekan orogeny was high enough to facilitate glaciations at that time. This could explain the discovery of ice rafted debris form the same period (Eldrett et al., 2007), previously thought to originate further southeast on Greenland (Eldrett et al., 2007; Vamvaka et al., 2019). Ice sheet models indicates that the Greenland topography should be 1–1.5 km higher than today to accommodate continental ice sheets in a warm Eocene climate (Langebroek et al., 2017), and this could have been true for the Eurekan orogeny (Vamvaka et al., 2019). Here we adopt elevations of ~2000 m for the Early Cenozoic, ~3000 m for the Late Eocene, before we gradually lower the topography.

5. Oceanic gateway events and their influence on paleo-ocean circulation and climate

The overall aim of our study is to construct a global digital model for the Cenozoic evolution of paleobathymetry, with a focus on the northern hemisphere oceanic gateways. We have indicated the importance of individual oceanic gateways and presented comprehensive and detailed paleobathymetric models for their respective regions. In the last section of this study we will re-iterate the importance of the oceanic gateways' evolution in modulating climate variations by reviewing the main climate change events since 66 Ma.

In the Early Cenozoic, the Southern Ocean gateways and the NE Atlantic were closed, and there was a deep circum-equatorial connection of the major oceanic basins through the CAS and the Tethys Ocean. From Late Eocene to Early Oligocene, this configuration changed as the Southern Ocean gateways opened, the GSR deepened through the FSC, and the Tethys Seaway shallowed. In the Miocene, the Tethys Seaway closed completely (Early–Mid Miocene), the CAS shallowed to values <1000 m (Mid–Miocene), the GSR deepened, punctuated by temporal episodes of uplift, and the Fram Strait approached modern depths (Mid–Miocene). The timing of the different gateways opening and closing with error bars representing the uncertainty in time based on published literature are summarized in Fig. 6. Their correlations with ocean circulation and climate changes are discussed below.

5.1. The Paleocene–Eocene

In the Early Eocene (Fig. 7), the CAS and Tethys Seaway were open, the North Atlantic was in an incipient stage, and the Southern Ocean gateways were closed (Fig. 6). In these conditions, the ocean circulation was influenced by deep water convection at multiple locations, including the North Pacific, southern high latitudes, and low-latitude regions producing warm saline deep water (Ferreira et al., 2018, and references therein). Compilations of Nd isotope data from ODP and IODP drillsites

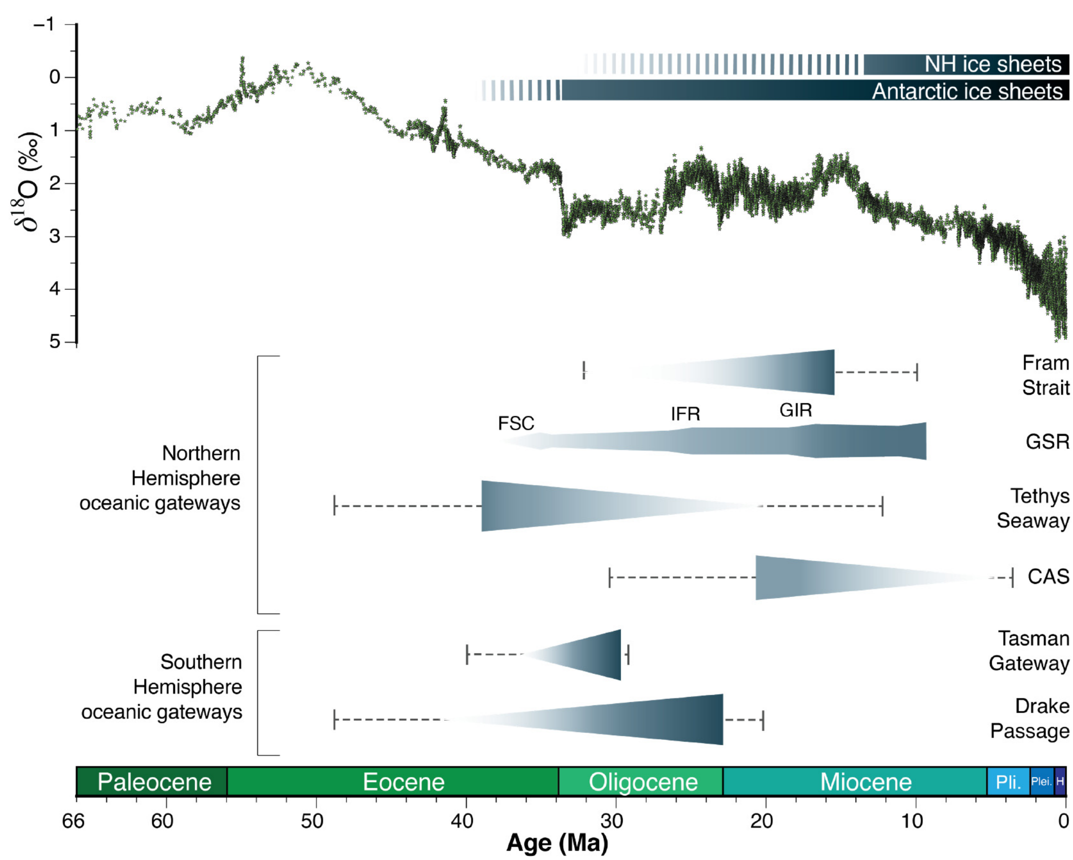

Fig. 6. Cenozoic deep sea benthic foraminifera oxygen isotope curve of Zachos et al. (2008) and timing of the key oceanic gateway changes considered in our model. Stapled error bars show the range of estimated times of oceanic gateways opening and closing from the literature. For the Fram Strait (i.e. Ehlers and Jokat, 2013; Jakobsson et al., 2007; Jokat et al., 2016; Knies and Gaina, 2008; Myhre et al., 1995b), for the GSR (i.e. Davies et al., 2001; Denk et al., 2011; Ellis and Stoker, 2014; Poore et al., 2006; Wold, 1995), for the Tethys Seaway (i.e. Allen and Armstrong, 2008; Dercourt et al., 1986; Oberhänsli, 1992; Okay et al., 2010; Rögl, 1999), for the CAS (i.e. Duque-Caro, 1990; Marshall et al., 1982; Montes et al., 2012a; Montes et al., 2015; Montes et al., 2012b), for the Tasman Gateway (Bijl et al., 2013; Brown et al., 2006; Stickley et al., 2004), and for the Drake Passage (Eagles and Jokat, 2014; Lawver and Gahagan, 2003; Lawver et al., 2011; Scher and Martin, 2006). FSC = Faroe Shetland Channel, IFR = Iceland–Faroe Ridge, GIR = Greenland–Iceland Ridge, GSR = Greenland–Scotland Ridge, CAS = Central American Seaway.

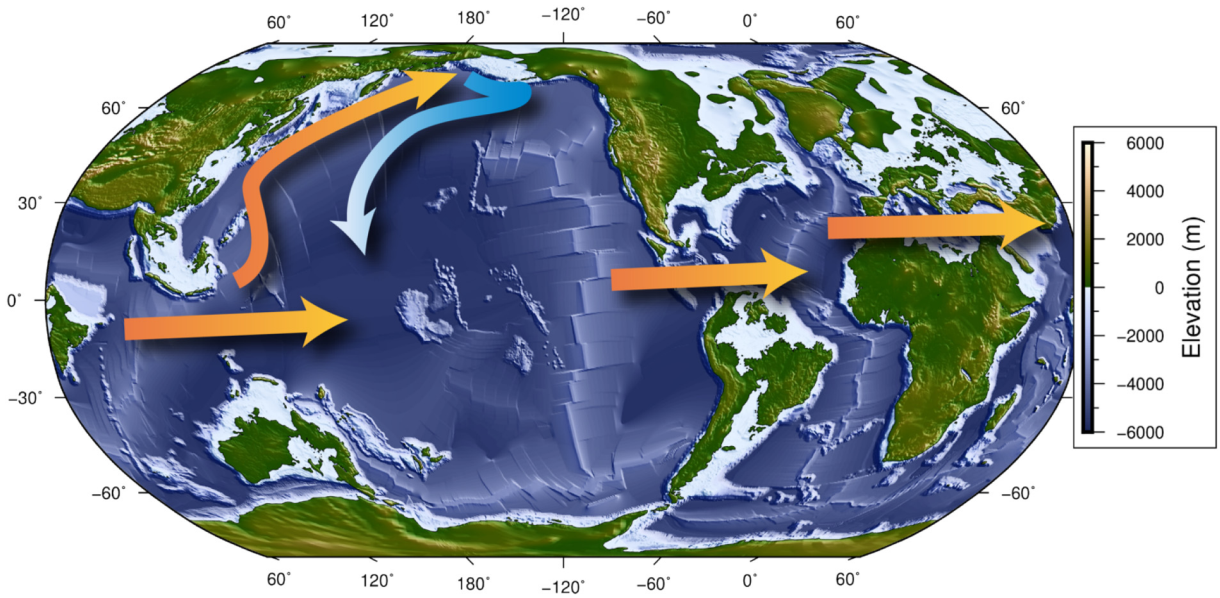

Fig. 7. Global paleobathymetry and paleotopography for the Early Eocene (55 Ma) with sketched ocean circulation pattern. Orange arrows = surface currents, blue arrows = deep water.

suggest separate overturning circulations in the Pacific and Atlantic Basins before ~40 Ma (Martin and Scher, 2004; Thomas et al., 2014). There was strong convection and deep water production in the Northern Pacific Ocean in the Early Cenozoic that started to weaken in the Early Eocene, possibly due to global warming (Hague et al., 2012). The tectonic configuration of oceanic basins was therefore important for the Early Eocene climate, by facilitating multiple regions of deep convection, younger water masses were produced in each basin, and overall increasing the ventilation (Thomas et al., 2014). This may have had important implications for carbon cycling, as higher ventilation rates could promote enhanced recycling of organic carbon, returning fixed carbon back to the ocean/atmosphere system as CO_2 (Hague et al., 2012; Olivarez Lyle and Lyle, 2006; Thomas et al., 2014). By the Late Eocene, the Southern Ocean gateways started to open, the GSR deepened, the Tethys Seaway shallowed (Fig. 5), and first indications of the initiation of the AMOC are found (e.g. Abelson and Erez, 2017; Coxall et al., 2018). It follows that these gateway events could have triggered climatic changes near the Eocene–Oligocene transition (see next section).

5.2. The Eocene Oligocene transition

Around the Eocene–Oligocene transition, the GSR opened through the FSC, and the Tethys Ocean started to get shallow and narrow, which could have influenced the changes in ocean circulation documented around that time. Tectonic changes in the Fram Strait and the Barents Sea, the GSR region and the Tethys Seaway have all been proposed as triggers for the Eocene–Oligocene cooling (Abelson and Erez, 2017; Coxall et al., 2018; Hutchinson et al., 2019; Zhang et al., 2011):

Recently, Hutchinson et al. (2019) proposed that a closing of an Atlantic–Arctic connection trough the Barents Sea before the EOT, could have enhanced the AMOC and contributed to the climatic cooling. Paleoenvironment and erosion estimates of the Barent Sea (e.g. Lasabuda et al., 2018) indicate a subaerial Barents Sea in the Eocene and Oligocene. There have been postulated periods of uplift in the Barents Sea indicating lower elevation in the Eocene relative to the Early Oligocene (Anell et al., 2009), but the amount of uplift and its influence on the topography is not certain. Our model does not include a submerged Barents Sea at that time as we implement a paleotopography similar to Lasabuda et al. (2018), and no late Eocene closure of a seaway through the Barents Sea. However, in our model we have a shallow water connection over the East Greenland margin in the Proto-Fram Strait. If this seaway was open earlier in the Eocene, uplift related to the second phase of the Eurekan Orogeny (e.g. Vamvaka et al., 2019) could have closed this connection to the Arctic Ocean and potentially influenced the circulation in the North Atlantic as suggested by Hutchinson et al. (2019).

Several studies argue for an onset of a stronger AMOC before or close to EOT because of paleobathymetric changes in the NE Atlantic region (Abelson et al., 2008; Abelson and Erez, 2017; Coxall et al., 2018). Abelson and Erez (2017) infer an onset of a modern-like AMOC near EOT deduced from compiled $\delta^{18}O$ and $\delta^{13}C$ benthic foraminifera records. They propose a hypothetical Nordic counterclockwise estuarine circulation route, where warm North Atlantic waters cross the GSR and enters the Eastern Nordic Seas, sinks in the Northern Nordic Seas, and returns though the FSC. This is consistent with the onset of deposition of the Southeast Faroe Drift at ~35 Ma (Davies et al., 2001). If there was deep water forming in the Nordic Seas at this time, the proposed circulation of Abelson and Erez (2017) seems plausible as indicated by our modelled paleobathymetry that shows the western part of the GSR subaerial and the FSC opened at this time.

The closure of the equatorial connection between the major oceanic basins through the CAS and the Tethys Seaway has been proposed to have impacted global ocean circulation and climate by causing a transition from a Southern Ocean Deep Water dominated circulation mode to a circulation dominated by North Atlantic Deep Water (Zhang et al., 2011). The CAS is thought to have been open at the EOT and gateway changes relevant for ocean circulation are believed to have occurred later (see Table 3). However, the Tethys Seaway may have closed at this time (Allen and Armstrong, 2008) and modelling suggests that it may have reduced deep water formation in the Southern Ocean, increased the AMOC, and caused cooling of high southern latitudes (Hamon et al., 2013; Zhang et al., 2011). In our paleobathymetry model, the Tethys Seaway is open, but it is no deeper than ~1000 m (Fig. 3). We cannot deduce solely from our paleobathymetry model how this gateway configuration modulated flow through the gateway. However, the modelling study of Hamon et al. (2013) shows that a 1000 m deep gateway would still export warm saline deep water to the Indian Ocean, but shallowing it to 250 m would terminate the presence of this water mass in the Indian Ocean. It follows that shallowing and narrowing of the Tethys Seaway in the Late Eocene and Early Oligocene could have made a difference to warm saline water transport, although ocean and

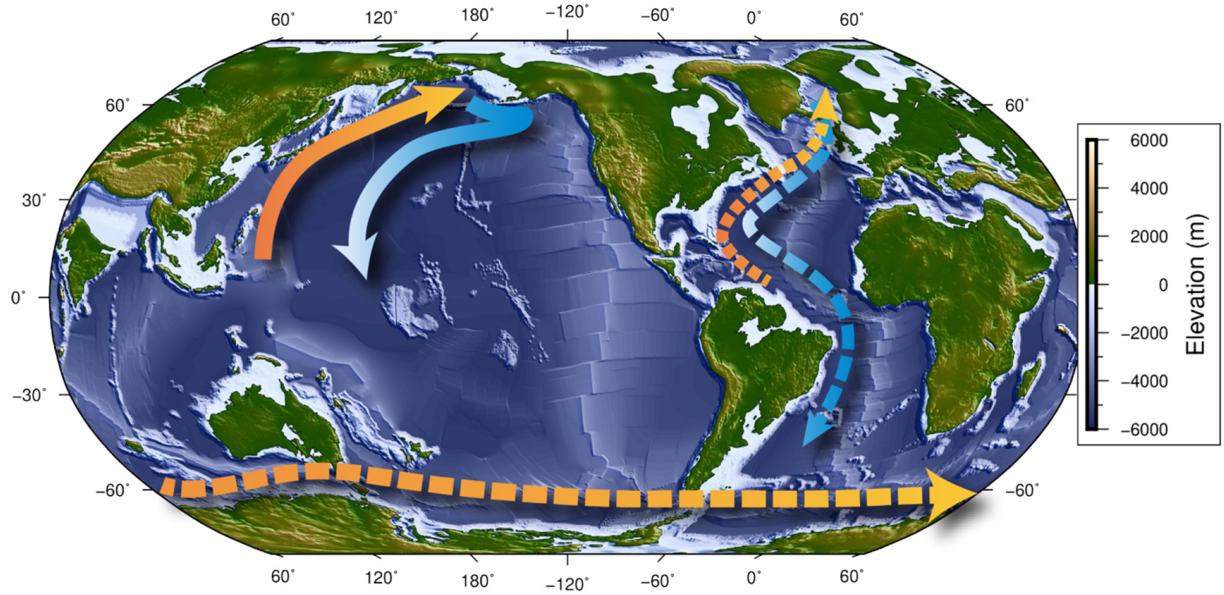

Fig. 8. Global paleobathymetry and paleotopography close to the Eocene–Oligocene transition (34 Ma) with sketched ocean circulation pattern. Orange arrows = surface currents, blue arrows = deep water.

climate models with realistic paleobathymetric reconstructions are required to constrain the gateways role (Fig. 8).

5.3. The Miocene

By the Mid-Miocene, the Fram Strait reached modern depths, Iceland appeared as an island as the GSR subsided, and the Tethys Seaway was closed (Fig. 9). The CAS was still open enabling exchange of Atlantic and Pacific waters, although it was narrowing, shallowing and possibly closing during this time (Montes et al., 2015). There was a warming trend in the Oligocene and Early Miocene culminating at the Mid-Miocene climatic optimum (~15 Ma) (Zachos et al., 2001). The transition to a cooler climate following the climatic optimum has been linked to oceanic circulation reorganization caused by final closure of the Tethys Seaway (Hamon et al., 2013). However, the Tethys Seaway probably closed several million years before this as major uplift is recorded in the Late Eocene (Allen and Armstrong, 2008). Further uplift and the consumption of the last oceanic lithosphere is documented in the Early Miocene (Okay et al., 2010), which is coeval with animal migration indicating a land-bridge across the seaway (Harzhauser et al., 2007). Instead we argue that CAS shallowing, GSR subsidence and uplift, or the deepening of the Fram Strait are more likely to have induced circulation changes in the Miocene. The modern AMOC started to develop in the Miocene (first stage was ~12–9 Ma), and during this time models and data suggests a weakening of the Pacific Meridional Overturning Circulation (PMOC) (e.g. Ferreira et al., 2018; von der Heydt and Dijkstra, 2006; Woodruff and Savin, 1989; Yang et al., 2014). CAS shallowing in the Miocene is believed to have strengthened the AMOC and changed the global ocean circulation pattern towards today's circulation system (e.g. Nisancioglu et al., 2003; Sepulchre et al., 2014). Also, temporal uplift and subsidence of GSR in the

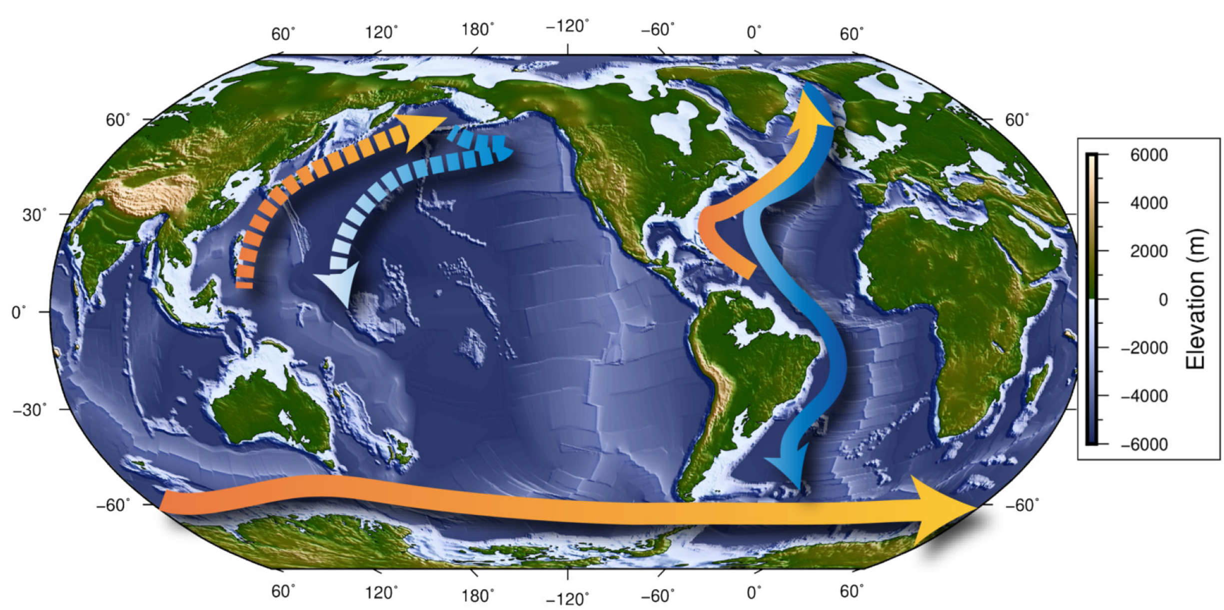

Fig. 9. Global paleobathymetry and paleotopography for the Mid Miocene (15 Ma) with sketched ocean circulation pattern. Orange arrows = surface currents, blue arrows = deep water.

Miocene has been linked to variations in the production of NCW and the Mid-Late Miocene cooling (e.g. Wright and Miller, 1996).

In addition, the deepening of the Fram Strait has been linked to ocean circulation changes and is postulated to have played a role in the climatic changes during the Miocene (Jakobsson et al., 2007; Knies and Gaina, 2008). In summary, the main major changes in NH gateways in our Miocene paleobathymetric model are the CAS shallowing from Early Miocene, depth variations of the GSR due to the Iceland plume pulsations throughout the Miocene, and Fram Strait deepening in the Early–Mid Miocene.

6. Summary and conclusions

We have developed a new model for Cenozoic paleobathymetry with a focus on the evolution of the Northern Hemisphere oceanic gateways. The model implements updated plate kinematics and associated oceanic lithospheric ages, estimated sediment thickness, and paleodepths of oceanic plateaus and microcontinents. In contrast to previous global models, we include a novel model for the NE Atlantic region that incorporates crustal thickness and variations in dynamic support from the Iceland mantle plume that greatly improves our reconstructions. In particular, the global model integrates regional reconstructions for the Northern Hemisphere oceanic gateways and is also complemented with a new paleotopography model that takes into account previously published geological information and reconstructed topography for selected regions.

We capture several tectonic and geodynamic events that changed the Northern Hemisphere oceanic gateways configuration through Cenozoic time. Due to plate tectonics and Iceland plume activity, the Greenland–Scotland Ridge gateway opens in the Late Eocene trough the FSC. Later on, the IFR deepens in the Early Oligocene, and Iceland becomes an island as the GIR submerge below sea level in the Mid Miocene. However, the subsidence history of the GSR experience temporal episodes of uplift related to changes in dynamic support from the Iceland Plume. In our global model, the Fram Strait evolves from a shallow connection to the Arctic Ocean in the Oligocene to modern depths (>2.5 km) by Early–Mid Miocene as the mid-ocean ridge between Greenland/North America and Eurasia is slowly connecting with the Gakkel Ridge in the Arctic Ocean. The Tethys Seaway is shallowing to ~1000 m in the Late Eocene, as the Arabian and Eurasian plates continue to converge, but does not close completely until the Early Miocene (~20 Ma). The Central American Seaway shallows in the Oligocene and Miocene and reach depths of less than ~500 m by Late Miocene. From Late Miocene, there are only very shallow (<250 m) and narrow (>~200 km) Atlantic–Pacific connections. Our up to date and detailed reconstructions, calculated at one million-year time step for the Cenozoic era, will be useful for the paleoclimate community as they can easily be implemented in paleo-ocean circulation and climate models.

Supplementary data to this article can be found online at https://doi.org/10.1016/j.gr.2020.05.011.

Declaration of competing interest

The authors declare that they have no known competing financial interests or personal relationships that could have appeared to influence the work reported in this paper.

Acknowledgements

E. S., C. G., S. M., and K.H.N. acknowledge support from the Research Council of Norway through its Centers of Excellence funding scheme, project 223272, and project 246929 (ClimVoTe). E. S. acknowledges support from the MatNat Faculty at the University of Oslo. We thank two anonymous reviewers for their constructive comments. The maps were generated using Generic Mapping Tools (GMT; Wessel et al., 2013), and perceptually uniform color maps were used in this study to prevent visual distortion of the data (Crameri, 2018a; Crameri, 2018b). For visualizing tectonic reconstructions, we have used the freely available software GPlates (gplates.org). The Cenozoic reconstructions are available here: https://doi.org/10.5281/zenodo.3820664.

References

Abbey, A.L., Niemi, N.A., Geissman, J.W., Winkelstern, I.Z., Heizler, M., 2017. Early Cenozoic exhumation and paleotopography in the Arkansas River valley, southern Rocky Mountains, Colorado. Lithosphere 10, 239–266.

Abelson, M., Erez, J., 2017. The onset of modern-like Atlantic meridional overturning circulation at the Eocene-Oligocene transition: evidence, causes, and possible implications for global cooling. Geochem. Geophys. Geosyst. 18, 2177–2199.

Abelson, M., Agnon, A., Almogi-Labin, A., 2008. Indications for control of the Iceland plume on the Eocene–Oligocene "greenhouse–icehouse" climate transition. Earth Planet. Sci. Lett. 265, 33–48.

Allen, M.B., Armstrong, H.A., 2008. Arabia–Eurasia collision and the forcing of mid-Cenozoic global cooling. Palaeogeogr. Palaeoclimatol. Palaeoecol. 265, 52–58.

Anell, I., Thybo, H., Artemieva, I.M., 2009. Cenozoic uplift and subsidence in the North Atlantic region: Geological evidence revisited. Tectonophysics 474, 78–105.

Baatsen, M., van Hinsbergen, D.J.J., von der Heydt, A.S., Dijkstra, H.A., Sluijs, A., Abels, H.A., Bijl, P.K., 2016. Reconstructing geographical boundary conditions for palaeoclimate modelling during the Cenozoic. Clim. Past 12, 1635–1644.

Beard, K.C., 2008. The oldest North American primate and mammalian biogeography during the Paleocene–Eocene Thermal Maximum. Proc. Natl. Acad. Sci. 105, 3815–3818.

Berggren, W., Schnitker, D., 1983. Cenozoic marine environments in the North Atlantic and Norwegian-Greenland Sea. Structure and Development of the Greenland-Scotland Ridge. Springer, pp. 495–548.

Bice, K.L., Marotzke, J., 2002. Could changing ocean circulation have destabilized methane hydrate at the Paleocene/Eocene boundary? Paleoceanography 17 (8-1-8-12).

Bijl, P.K., Bendle, J.A., Bohaty, S.M., Pross, J., Schouten, S., Tauxe, L., Stickley, C.E., McKay, R.M., Röhl, U., Olney, M., 2013. Eocene cooling linked to early flow across the Tasmanian Gateway. Proc. Natl. Acad. Sci. 110, 9645–9650.

Broecker, W., Peacock, S., Walker, S., Weiss, R., Fahrbach, E., Schröder, M., Mikolajewicz, U., Heinze, C., Key, R., Peng, T.H., 1998. How much deep water is formed in the Southern Ocean? Journal of Geophysical Research: Oceans 103, 15833–15843.

Brown, B., Gaina, C., Müller, R.D., 2006. Circum-Antarctic palaeobathymetry: illustrated examples from Cenozoic to recent times. Palaeogeogr. Palaeoclimatol. Palaeoecol. 231, 158–168.

Cao, W., Zahirovic, S., Flament, N., Williams, S.E., Golonka, J., Muller, R.D., 2017. Improving Global Paleogeography Since the Late Paleozoic Using Paleobiology.

Chamberlain, C.P., Mix, H.T., Mulch, A., Hren, M.T., Kent-Corson, M.L., Davis, S.J., Horton, T.W., Graham, S.A., 2012. The Cenozoic climatic and topographic evolution of the western North American Cordillera. Am. J. Sci. 312, 213–262.

Clift, P.D., Turner, J., 1995. Dynamic support by the Iceland Plume and its effect on the subsidence of the northern Atlantic margins. J. Geol. Soc. 152, 935–941.

Cocks, L.R.M., Torsvik, T.H., 2016. Methods for locating old continents and terranes. In: Cocks, L.R.M., Torsvik, T.H. (Eds.), Earth History and Palaeogeography. Cambridge University Press, Cambridge, pp. 1–2.

Coleman, M., Hodges, K., 1995. Evidence for Tibetan plateau uplift before 14 Myr ago from a new minimum age for east–west extension. Nature 374, 49–52.

Conrad, C.P., 2013. The solid Earth's influence on sea level. GSA Bull. 125, 1027–1052.

Coxall, H.K., Huck, C.E., Huber, M., Lear, C.H., Legarda-Lisarri, A., O'Regan, M., Sliwinska, K.K., van de Flierdt, T., de Boer, A.M., Zachos, J.C., Backman, J., 2018. Export of nutrient rich Northern Component Water preceded early Oligocene Antarctic glaciation. Nat. Geosci. 11, 190–196.

Cramer, B.S., Miller, K.G., Barrett, P.J., Wright, J.D., 2011. Late Cretaceous–Neogene trends in deep ocean temperature and continental ice volume: reconciling records of benthic foraminiferal geochemistry (δ^{18}O and Mg/Ca) with sea level history. Journal of Geophysical Research: Oceans 116.

Crameri, F., 2018a. Geodynamic diagnostics, scientific visualisation and StagLab 3.0. Geosci. Model Dev. 11, 2541–2562.

Crameri, F., 2018b. Scientific Colour-maps.

Crosby, A.G., McKenzie, D., 2009. An analysis of young ocean depth, gravity and global residual topography. Geophys. J. Int. 178, 1198–1219.

Crosby, A., McKenzie, D., Sclater, J., 2006. The relationship between depth, age and gravity in the oceans. Geophys. J. Int. 166, 553–573.

Davies, R., Cartwright, J., Pike, J., Line, C., 2001. Early Oligocene initiation of North Atlantic deep water formation. Nature 410, 917–920.

De Paor, D.G., Bradley, D.C., Eisenstadt, G., Phillips, S.M., 1989. The Arctic Eurekan orogen: a most unusual fold-and-thrust belt. GSA Bull. 101, 952–967.

DeConto, R.M., Pollard, D., 2003. Rapid Cenozoic glaciation of Antarctica induced by declining atmospheric CO_2. Nature 421, 245–249.

Denk, T., Grímsson, F., Zetter, R., Símonarson, L.A., 2011. The Biogeographic History of Iceland–The North Atlantic Land Bridge Revisited, Late Cainozoic floras of Iceland. Springer, pp. 647–668.

Dercourt, J., Zonenshain, L.P., Ricou, L.E., Kazmin, V.G., Le Pichon, X., Knipper, A.L., Grandjacquet, C., Sbortshikov, I.M., Geyssant, J., Lepvrier, C., Pechersky, D.H., Boulin, J., Sibuet, J.C., Savostin, L.A., Sorokhtin, O., Westphal, M., Bazhenov, M.L., Lauer, J.P., Biju-Duval, B., 1986. Geological evolution of the Tethys belt from the Atlantic to the Pamirs since the LIAS. Tectonophysics 123, 241–315.

Dimakis, P., Braathen, B.I., Faleide, J.I., Elverhøi, A., Gudlaugsson, S.T., 1998. Cenozoic erosion and the preglacial uplift of the Svalbard–Barents Sea region. Tectonophysics 300, 311–327.
Doubrovine, P.V., Steinberger, B., Torsvik, T.H., 2012. Absolute plate motions in a reference frame defined by moving hot spots in the Pacific, Atlantic, and Indian oceans. Journal of Geophysical Research: Solid Earth 117.
Duque-Caro, H., 1990. Neogene stratigraphy, paleoceanography and paleobiogeography in northwest South America and the evolution of the Panama Seaway. Palaeogeogr. Palaeoclimatol. Palaeoecol. 77, 203–234.
Dutkiewicz, A., Müller, R.D., Wang, X., O'Callaghan, S., Cannon, J., Wright, N.M., 2017. Predicting sediment thickness on vanished ocean crust since 200 Ma. Geochem. Geophys. Geosyst. 18, 4586–4603.
Eagles, G., Jokat, W., 2014. Tectonic reconstructions for paleobathymetry in Drake Passage. Tectonophysics 611, 28–50.
Ehlers, B.-M., Jokat, W., 2013. Paleo-bathymetry of the northern North Atlantic and consequences for the opening of the Fram Strait. Mar. Geophys. Res. 34, 25–43.
Eldrett, J.S., Harding, I.C., Wilson, P.A., Butler, E., Roberts, A.P., 2007. Continental ice in Greenland during the Eocene and Oligocene. Nature 446, 176–179.
Ellis, D., Stoker, M.S., 2014. The Faroe–Shetland Basin: a regional perspective from the Paleocene to the present day and its relationship to the opening of the North Atlantic Ocean. Geol. Soc. Lond., Spec. Publ. 397, 11–31.
Elsworth, G., Galbraith, E., Halverson, G., Yang, S., 2017. Enhanced Weathering and CO_2 Drawdown Caused by Latest Eocene Strengthening of the Atlantic Meridional Overturning Circulation. Nature Geosci Advance Online Publication.
Engen, Ø., Faleide, J.I., Dyreng, T.K., 2008. Opening of the Fram Strait gateway: a review of plate tectonic constraints. Tectonophysics 450, 51–69.
Ferreira, D., Cessi, P., Coxall, H.K., Boer, A.d., Dijkstra, H.A., Drijfhout, S.S., Eldevik, T., Harnik, N., McManus, J.F., Marshall, D.P., Nilsson, J., Roquet, F., Schneider, T., Wills, R.C., 2018. Atlantic-Pacific asymmetry in deep water formation. Annu. Rev. Earth Planet. Sci. 46, 327–352.
Funck, T., Geissler, W.H., Kimbell, G.S., Gradmann, S., Erlendsson, Ö., McDermott, K., Petersen, U.K., 2017. Moho and basement depth in the NE Atlantic Ocean based on seismic refraction data and receiver functions. Geol. Soc. Lond., Spec. Publ. 447, 207–231.
Gaina, C., Jakob, J., 2018. Global Eocene tectonic unrest: possible causes and effects around the North American plate. Tectonophysics 760, 136–151.
Gaina, C., Torsvik, T.H., van Hinsbergen, D.J., Medvedev, S., Werner, S.C., Labails, C., 2013. The African Plate: a history of oceanic crust accretion and subduction since the Jurassic. Tectonophysics 604, 4–25.
Gaina, C., Hinsbergen, D.J., Spakman, W., 2015. Tectonic interactions between India and Arabia since the Jurassic reconstructed from marine geophysics, ophiolite geology, and seismic tomography. Tectonics 34, 875–906.
Gaina, C., Nasuti, A., Kimbell, G.S., Blischke, A., 2017. Break-up and Seafloor Spreading Domains in the NE Atlantic. vol. 447, SP447. Geological Society, London, Special Publications, p. 412.
Gelati, R., 1975. Miocene marine sequence from Lake Van, eastern Turkey. Riv. Ital. Paleontol. Stratigr. 81, 477–490.
Goswami, A., Olson, P., Hinnov, L., Gnanadesikan, A., 2015. OESbathy version 1.0: a method for reconstructing ocean bathymetry with generalized continental shelf-slope-rise structures. Geosci. Model Dev. 8, 2735–2748.
Hague, A.M., Thomas, D.J., Huber, M., Korty, R., Woodard, S.C., Jones, L.B., 2012. Convection of North Pacific deep water during the early Cenozoic. Geology 40, 527–530.
Hamon, N., Sepulchre, P., Lefebvre, V., Ramstein, G., 2013. The role of eastern Tethys seaway closure in the Middle Miocene Climatic Transition (ca. 14 Ma). Clim. Past 9, 2687–2702.
Haq, B.U., Al-Qahtani, A.M., 2005. Phanerozoic cycles of sea-level change on the Arabian Platform. GeoArabia 10, 127–160.
Hartz, E.H., Medvedev, S., Schmid, D.W., 2017. Development of sedimentary basins: differential stretching, phase transitions, shear heating and tectonic pressure. Basin Res. 29, 591–604.
Harzhauser, M., Kroh, A., Mandic, O., Piller, W.E., Göhlich, U., Reuter, M., Berning, B., 2007. Biogeographic responses to geodynamics: a key study all around the Oligo–Miocene Tethyan Seaway. Zoologischer Anzeiger-A Journal of Comparative Zoology 246, 241–256.
Haug, G.H., Tiedemann, R., Zahn, R., Ravelo, A.C., 2001. Role of Panama uplift on oceanic freshwater balance. Geology 29, 207–210.
Herold, N., Seton, M., Müller, R., You, Y., Huber, M., 2008. Middle Miocene tectonic boundary conditions for use in climate models. Geochem. Geophys. Geosyst. 9.
Herold, N., Buzan, J., Seton, M., Goldner, A., Green, J.A.M., Müller, R.D., Markwick, P., Huber, M., 2014. A suite of early Eocene (~55 Ma) climate model boundary conditions. Geosci. Model Dev. 7, 2077–2090.
Hohbein, M.W., Sexton, P.F., Cartwright, J.A., 2012. Onset of North Atlantic Deep Water production coincident with inception of the Cenozoic global cooling trend. Geology 40, 255–258.
Holland, W.R., 1973. Baroclinic and topographic influences on the transport in western boundary currents. Geophysical Fluid Dynamics 4, 187–210.
Hoorn, C., Wesselingh, F.P., ter Steege, H., Bermudez, M.A., Mora, A., Sevink, J., Sanmartín, I., Sanchez-Meseguer, A., Anderson, C.L., Figueiredo, J.P., Jaramillo, C., Riff, D., Negri, F.R., Hooghiemstra, H., Lundberg, J., Stadler, T., Särkinen, T., Antonelli, A., 2010. Amazonia through time: Andean uplift, climate change, landscape evolution, and biodiversity. Science 330, 927–931.
Hüsing, S.K., Zachariasse, W.-J., van Hinsbergen, D.J.J., Krijgsman, W., Inceöz, M., Harzhauser, M., Mandic, O., Kroh, A., 2009. Oligocene–Miocene basin evolution in SE Anatolia, Turkey: constraints on the closure of the eastern Tethys gateway. Geol. Soc. Lond., Spec. Publ. 311, 107–132.
Hutchinson, D.K., Coxall, H.K., O'Regan, M., Nilsson, J., Caballero, R., de Boer, A.M., 2019. Arctic closure as a trigger for Atlantic overturning at the Eocene-Oligocene transition. Nat. Commun. 10, 3797.
Jakobsson, M., Backman, J., Rudels, B., Nycander, J., Frank, M., Mayer, L., Jokat, W., Sangiorgi, F., O'Regan, M., Brinkhuis, H., King, J., Moran, K., 2007. The early Miocene onset of a ventilated circulation regime in the Arctic Ocean. Nature 447, 986–990.
Jokat, W., Lehmann, P., Damaske, D., Bradley Nelson, J., 2016. Magnetic signature of North-East Greenland, the Morris Jesup Rise, the Yermak Plateau, the central Fram Strait: Constraints for the rift/drift history between Greenland and Svalbard since the Eocene. Tectonophysics 691, 98–109.
Jolivet, L., Faccenna, C., 2000. Mediterranean extension and the Africa-Eurasia collision. Tectonics 19, 1095–1106.
Jones M, S., White, N., 2003. Shape and size of the starting Iceland plume swell. Earth Planet. Sci. Lett. 216 (3), 271–282. https://doi.org/10.1016/S0012-821X(03)00507-7.
Jones, S.M., White, N., Maclennan, J., 2002. V-shaped ridges around Iceland: implications for spatial and temporal patterns of mantle convection. Geochem. Geophys. Geosyst. 3, 1–23.
Jones, S.M., Murton, B.J., Fitton, J.G., White, N.J., Maclennan, J., Walters, R.L., 2014. A joint geochemical–geophysical record of time-dependent mantle convection south of Iceland. Earth Planet. Sci. Lett. 386, 86–97.
Kaminski, M.A., Silye, L.r.n., Kender, S., 2005. Miocene deep-water agglutinated foraminifera from ODP Hole 909c: implications for the paleoceanography of the Fram Strait Area, Greenland Sea. Micropaleontology 51, 373–403.
Karas, C., Nürnberg, D., Bahr, A., Groeneveld, J., Herrle, J.O., Tiedemann, R., deMenocal, P.B., 2017. Pliocene oceanic seaways and global climate. Sci. Rep. 7, 39842.
Karlsen, K.S., Conrad, C.P., Magni, V., 2019. Deep water cycling and sea level change since the breakup of Pangea. Geochem. Geophys. Geosyst. 20, 2919–2935.
Karlsen, K.S., Domeier, M., Gaina, C., Conrad, C.P., 2020. A tracer-based algorithm for automatic generation of seafloor age grids from plate tectonic reconstructions. Comput. Geosci. 140, 104508.
Kennett, J.P., 1977. Cenozoic evolution of Antarctic glaciation, the circum-Antarctic Ocean, and their impact on global paleoceanography. J. Geophys. Res. 82, 3843–3860.
Knies, J., Gaina, C., 2008. Middle Miocene ice sheet expansion in the Arctic: views from the Barents Sea. Geochem. Geophys. Geosyst. 9.
Knies, J., Mattingsdal, R., Fabian, K., Grøsfjeld, K., Baranwal, S., Husum, K., De Schepper, S., Vogt, C., Andersen, N., Matthiessen, J., 2014. Effect of early Pliocene uplift on late Pliocene cooling in the Arctic–Atlantic gateway. Earth Planet. Sci. Lett. 387, 132–144.
Kristoffersen, Y., 1990. On the Tectonic Evolution and Paleoceanographic Significance of the Fram Strait Gateway, Geological History of the Polar Oceans: Arctic Versus Antarctic. Springer, pp. 63–76.
Langebroek, P.M., Nisancioglu, K.H., Lunt, D.J., Kathrine Pedersen, V., Nele Meckler, A., Gasson, E., 2017. On the possibility of ice on Greenland during the Eocene-Oligocene transition. EGU General Assembly Conference Abstracts, p. 3163.
Lasabuda, A., Laberg, J.S., Knutsen, S.-M., Høgseth, G., 2018. Early to middle Cenozoic paleoenvironment and erosion estimates of the southwestern Barents Sea: insights from a regional mass-balance approach. Mar. Pet. Geol. 96, 501–521.
Lawver, L.A., Gahagan, L.M., 2003. Evolution of Cenozoic seaways in the circum-Antarctic region. Palaeogeogr. Palaeoclimatol. Palaeoecol. 198, 11–37.
Lawver, L., Müller, D., 1994. Iceland hotspot track. Geol. 22 (4), 311–314. https://doi.org/10.1130/0091-7613(1994)022<0311:IHT>2.3.CO;2.
Lawver, L.A., Gahagan, L.M., Dalziel, I.W., 2011. A different look at gateways: Drake Passage and Australia/Antarctica. Tectonic, climatic, and cryospheric evolution of the Antarctic Peninsula 5–33.
Lear, C.H., Rosenthal, Y., Wright, J.D., 2003. The closing of a seaway: ocean water masses and global climate change. Earth Planet. Sci. Lett. 210, 425–436.
Livermore, R., Nankivell, A., Eagles, G., Morris, P., 2005. Paleogene opening of Drake passage. Earth Planet. Sci. Lett. 236, 459–470.
Maier-Reimer, E., Mikolajewicz, U., Crowley, T., 1990. Ocean general circulation model sensitivity experiment with an open Central American Isthmus. Paleoceanography 5, 349–366.
Marincovich, L., Gladenkov, A.Y., 2001. New evidence for the age of Bering Strait. Quat. Sci. Rev. 20, 329–335.
Markwick, P.J., Valdes, P.J., 2004. Palaeo-digital elevation models for use as boundary conditions in coupled ocean–atmosphere GCM experiments: a Maastrichtian (late Cretaceous) example. Palaeogeogr. Palaeoclimatol. Palaeoecol. 213, 37–63.
Marshall, L.G., Webb, S.D., Sepkoski, J.J., Raup, D.M., 1982. Mammalian evolution and the great American interchange. Science 215, 1351–1357.
Martin, E.E., Scher, H.D., 2004. Preservation of seawater Sr and Nd isotopes in fossil fish teeth: bad news and good news. Earth Planet. Sci. Lett. 220, 25–39.
Matthiessen, J., Brinkhuis, H., Poulsen, N., Smelror, M., 2009. Decahedrella martinheadii Manum 1997 - a stratigraphically and paleoenvironmentally useful Miocene acritarch of the high northern latitudes. Micropaleontology 55, 171–186.
Mauritzen, C., 1996. Production of dense overflow waters feeding the North Atlantic across the Greenland-Scotland Ridge. Part 1: evidence for a revised circulation scheme. Deep-Sea Res. I Oceanogr. Res. Pap. 43, 769–806.
McKenna, M.C., 1983a. Cenozoic paleogeography of North Atlantic land bridges. Structure and Development of the Greenland-Scotland Ridge. Springer, pp. 351–399.
McKenna, M.C., 1983b. Holarctic landmass rearrangement, cosmic events, and Cenozoic terrestrial organisms. Ann. Mo. Bot. Gard. 459–489.
Medvedev, S., Hartz, E.H., Faleide, J.I., 2018. Erosion-driven vertical motions of the circum Arctic: comparative analysis of modern topography. J. Geodyn. 119, 62–81.
Miller, K.G., Kominz, M.A., Browning, J.V., Wright, J.D., Mountain, G.S., Katz, M.E., Sugarman, P.J., Cramer, B.S., Christie-Blick, N., Pekar, S.F., 2005. The Phanerozoic record of global sea-level change. Science 310, 1293–1298.

Molnar, P., 2004. Late Cenozoic increase in accumulation rates of terrestrial sediment: how might climate change have affected erosion rates? Annu. Rev. Earth Planet. Sci. 32, 67–89.
Montes, C., Bayona, G., Cardona, A., Buchs, D.M., Silva, C., Morón, S., Hoyos, N., Ramírez, D., Jaramillo, C., Valencia, V., 2012a. Arc-continent collision and orocline formation: closing of the central American seaway. Journal of Geophysical Research: Solid Earth 117.
Montes, C., Cardona, A., McFadden, R., Morón, S.E., Silva, C.A., Restrepo-Moreno, S., Ramírez, D.A., Hoyos, N., Wilson, J., Farris, D., Bayona, G.A., Jaramillo, C.A., Valencia, V., Bryan, J., Flores, J.A., 2012b. Evidence for middle Eocene and younger land emergence in central Panama: implications for Isthmus closure. GSA Bull. 124, 780–799.
Montes, C., Cardona, A., Jaramillo, C., Pardo, A., Silva, J., Valencia, V., Ayala, C., Pérez-Angel, L., Rodriguez-Parra, L., Ramirez, V., 2015. Middle miocene closure of the Central American seaway. Science 348, 226–229.
Müller, R.D., Sdrolias, M., Gaina, C., Steinberger, B., Heine, C., 2008. Long-term sea-level fluctuations driven by ocean basin dynamics. Science 319, 1357–1362.
Myhre, A., Thiede, J., Firth, J., 1995a. 1. North Atlantic-Arctic gateways. Proceedings Ocean Drilling Program Initial Reports.
Myhre, A., Thiede, J., Firth, J., Ahagon, N., Black, K., Bloemendal, J., Brass, G., Bristow, J., Chow, N., Cremer, M., 1995b. Site 909, Proceedings of the Ocean Drilling Program. Initial Reports. Ocean Drilling Program. pp. 159–220.
Newkirk, D.R., Martin, E.E., 2009. Circulation through the Central American Seaway during the Miocene carbonate crash. Geology 37, 87–90.
Nikishin, A., Gaina, C., Petrov, E., Malyshev, N., Freiman, S., 2017. Eurasia Basin and Gakkel Ridge, Arctic Ocean: crustal asymmetry, ultra-slow spreading and continental rifting revealed by new seismic data. Tectonophysics 746, 64–82.
Nisancioglu, K.H., Raymo, M.E., Stone, P.H., 2003. Reorganization of Miocene deep water circulation in response to the shoaling of the Central American Seaway. Paleoceanography 18.
Oberhänsli, H., 1992. The influence of the Tethys on the bottom waters of the early Tertiary ocean. The Antarctic Paleoenvironment: A Perspective on Global Change: Part One 167–184.
Okay, A.I., Zattin, M., Cavazza, W., 2010. Apatite fission-track data for the Miocene Arabia-Eurasia collision. Geology 38, 35–38.
Olivarez Lyle, A., Lyle, M.W., 2006. Missing organic carbon in Eocene marine sediments: is metabolism the biological feedback that maintains end-member climates? Paleoceanography 21.
Olson, P., Reynolds, E., Hinnov, L., Goswami, A., 2016. Variation of ocean sediment thickness with crustal age. Geochem. Geophys. Geosyst. 17, 1349–1369.
Osborne, A.H., Newkirk, D.R., Groeneveld, J., Martin, E.E., Tiedemann, R., Frank, M., 2014. The seawater neodymium and lead isotope record of the final stages of Central American Seaway closure. Paleoceanography 29, 715–729.
Pagani, M., Huber, M., Liu, Z., Bohaty, S.M., Henderiks, J., Sijp, W., Krishnan, S., DeConto, R.M., 2011. The role of carbon dioxide during the onset of antarctic glaciation. Science 334, 1261–1264.
Parnell-Turner, R., White, N., Henstock, T., Murton, B., Maclennan, J., Jones, S.M., 2014. A continuous 55-million-year record of transient mantle plume activity beneath Iceland. Nat. Geosci. 7, 914–919.
Paxman, G.J.G., Jamieson, S.S.R., Hochmuth, K., Gohl, K., Bentley, M.J., Leitchenkov, G., Ferraccioli, F., 2019. Reconstructions of Antarctic topography since the Eocene–Oligocene boundary. Palaeogeogr. Palaeoclimatol. Palaeoecol. 535, 109346.
Polzin, K.L., Toole, J.M., Ledwell, J.R., Schmitt, R.W., 1997. Spatial variability of turbulent mixing in the abyssal ocean. Science 276, 93–96.
Poore, H., Samworth, R., White, N., Jones, S., McCave, I., 2006. Neogene overflow of northern component water at the Greenland-Scotland Ridge. Geochem. Geophys. Geosyst. 7.
Ramsay, A.T., Smart, C.W., Zachos, J.C., 1998. A model of early to middle Miocene deep ocean circulation for the Atlantic and Indian Oceans. Geol. Soc. Lond., Spec. Publ. 131, 55–70.
Rasmussen, E., Fjeldskaar, W., 1996. Quantification of the Pliocene-Pleistocene erosion of the Barents Sea from present-day bathymetry. Glob. Planet. Chang. 12, 119–133.
Raymo, M.E., 1994. The Himalayas, organic carbon burial, and climate in the Miocene. Paleoceanography 9, 399–404.
Raymo, M.E., Ruddiman, W.F., Froelich, P.N., 1988. Influence of late Cenozoic mountain building on ocean geochemical cycles. Geology 16, 649–653.
Rebesco, M., Hernández-Molina, F.J., Van Rooij, D., Wåhlin, A., 2014. Contourites and associated sediments controlled by deep-water circulation processes: state-of-the-art and future considerations. Mar. Geol. 352, 111–154.
Reuter, M., Piller, W.E., Harzhauser, M., Mandic, O., Berning, B., Rögl, F., Kroh, A., Aubry, M.-P., Wielandt-Schuster, U., Hamedani, A., 2009. The Oligo-/Miocene Qom Formation (Iran): evidence for an early Burdigalian restriction of the Tethyan Seaway and closure of its Iranian gateways. Int. J. Earth Sci. 98, 627–650.
Robertson, A.H.F., Parlak, O., Rízaoğlu, T., Ünlügenç, Ü., İnan, N., Tasli, K., Ustaömer, T., 2007. Tectonic evolution of the South Tethyan ocean: evidence from the Eastern Taurus Mountains (Elaziğ region, SE Turkey). Geol. Soc. Lond., Spec. Publ. 272, 231–270.
Rögl, F., 1999. Mediterranean and Paratethys. Facts and hypotheses of an Oligocene to Miocene paleogeography (short overview). Geol. Carpath. 50, 339–349.
Rowley, D.B., Currie, B.S., 2006. Palaeo-altimetry of the late Eocene to Miocene Lunpola basin, central Tibet. Nature 439, 677–681.
Scher, H.D., Martin, E.E., 2006. Timing and climatic consequences of the opening of Drake Passage. Science 312, 428–430.
Scher, H.D., Whittaker, J.M., Williams, S.E., Latimer, J.C., Kordesch, W.E., Delaney, M.L., 2015. Onset of Antarctic Circumpolar Current 30 million years ago as Tasmanian Gateway aligned with westerlies. Nature 523, 580–583.
Sepulchre, P., Arsouze, T., Donnadieu, Y., Dutay, J.C., Jaramillo, C., Le Bras, J., Martin, E., Montes, C., Waite, A., 2014. Consequences of shoaling of the Central American Seaway determined from modeling Nd isotopes. Paleoceanography 29, 176–189.
Seton, M., Müller, R., Zahirovic, S., Gaina, C., Torsvik, T., Shephard, G., Talsma, A., Gurnis, M., Turner, M., Maus, S., 2012. Global continental and ocean basin reconstructions since 200Ma. Earth Sci. Rev. 113, 212–270.
Sijp, W.P., England, M.H., Huber, M., 2011. Effect of the deepening of the Tasman Gateway on the global ocean. Paleoceanography 26.
Sijp, W.P., von der Heydt, A.S., Dijkstra, H.A., Flögel, S., Douglas, P.M.J., Bijl, P.K., 2014. The role of ocean gateways on cooling climate on long time scales. Glob. Planet. Chang. 119, 1–22.
Stein, C.A., Stein, S., 1992. A model for the global variation in oceanic depth and heat flow with lithospheric age. Nature 359, 123–129.
Stickley, C.E., Brinkhuis, H., Schellenberg, S.A., Sluijs, A., Röhl, U., Fuller, M., Grauert, M., Huber, M., Warnaar, J., Williams, G.L., 2004. Timing and nature of the deepening of the Tasmanian Gateway. Paleoceanography 19.
Stoker, M.S., Hoult, R.J., Nielsen, T., Hjelstuen, B.O., Laberg, J.S., Shannon, P.M., Praeg, D., Mathiesen, A., van Weering, T.C.E., McDonnell, A., 2005. Sedimentary and oceanographic responses to early Neogene compression on the NW European margin. Mar. Pet. Geol. 22, 1031–1044.
Stoker, M., Leslie, A., Smith, K., Ólavsdóttir, J., Johnson, H., Laberg, J.S., 2013. Onset of North Atlantic Deep Water production coincident with inception of the Cenozoic global cooling trend: comment. Geology 41 e291-e291.
Straume, E.O., Gaina, C., Medvedev, S., Hochmuth, K., Gohl, K., Whittaker, J.M., Abdul Fattah, R., Doornenbal, J.C., Hopper, J.R., 2019. GlobSed: updated total sediment thickness in the world's oceans. Geochem. Geophys. Geosyst. 20, 1756–1772.
Sykes, T.J.S., 1996. A correction for sediment load upon the ocean floor: uniform versus varying sediment density estimations—implications for isostatic correction. Mar. Geol. 133, 35–49.
Talwani, M., Gleb, U., Kjell, Bjorklund, Caston, V.N.D., Faas, Richard W., van Hinte, Jan E., Kharin, G.N., Morris, David A., Müller, Carla, Nilsen, Tor H., Warnke, Detlef A., White, a.S.M., 1976. Initial Reports of the Deep Sea Drilling Project. vol. 38. US Government Printing Office, Dublin, Ireland to Amsterdam, The Netherlands.
Thiede, J., Eldholm, O., 1983. Speculations about the Paleodepth of the Greenland-Scotland Ridge during late Mesozoic and Cenozoic times. In: Bott, M.H.P., Saxov, S., Talwani, M., Thiede, J. (Eds.), Structure and Development of the Greenland-Scotland Ridge: New Methods and Concepts. Springer US, Boston, MA, pp. 445–456.
Thiede, J., Myhre, A.M., 1996. 36. The palaeoceanographic history of the North Atlantic–Arctic gateways: synthesis of the Leg 151 drilling results. Proceedings of the Ocean Drilling Program, Scientific Results. Citeseer, pp. 645–658.
Thomas, D.J., Korty, R., Huber, M., Schubert, J.A., Haines, B., 2014. Nd isotopic structure of the Pacific Ocean 70–30 Ma and numerical evidence for vigorous ocean circulation and ocean heat transport in a greenhouse world. Paleoceanography 29, 454–469.
Toggweiler, J., Samuels, B., 1995. Effect of Drake Passage on the global thermohaline circulation. Deep-Sea Res. I Oceanogr. Res. Pap. 42, 477–500.
Torsvik, T.H., Cocks, L.R.M., 2016. Tectonic units of the Earth. In: Cocks, L.R.M., Torsvik, T.H. (Eds.), Earth History and Palaeogeography. Cambridge University Press, Cambridge, pp. 38–76.
Vamvaka, A., Pross, J., Monien, P., Piepjohn, K., Estrada, S., Lisker, F., Spiegel, C., 2019. Exhuming the top end of North America: episodic evolution of the Eurekan belt and its potential relationships to North Atlantic plate tectonics and Arctic climate change. Tectonics 0.
van Hinsbergen, D.J.J., Torsvik, T.H., Schmid, S.M., Maţenco, L.C., Maffione, M., Vissers, R.L.M., Gürer, D., Spakman, W., 2019. Orogenic architecture of the Mediterranean region and kinematic reconstruction of its tectonic evolution since the Triassic. Gondwana Res. 81, 79–229.
von der Heydt, A., Dijkstra, H.A., 2006. Effect of ocean gateways on the global ocean circulation in the late Oligocene and early Miocene. Paleoceanography 21.
Wang, C., Li, X., Hu, X., Jansa, L.F., 2002. Latest marine horizon north of Qomolangma (Mt Everest): implications for closure of Tethys seaway and collision tectonics. Terra Nova 14, 114–120.
Webb, S.D., 2006. The great American biotic interchange: patterns and processes. Ann. Mo. Bot. Gard. 245–257.
Wessel, P., Smith, W.H., Scharroo, R., Luis, J., Wobbe, F., 2013. Generic mapping tools: improved version released. Eos, Transactions American Geophysical Union 94, 409–410.
White, R., McKenzie, D., 1989. Magmatism at rift zones: the generation of volcanic continental margins and flood basalts. J. Geophys. Res. Solid Earth 94 (B6), 7685–7729. https://doi.org/10.1029/JB094iB06p07685.
White, R.S., McKenzie, D., O'Nions, R.K., 1992. Oceanic crustal thickness from seismic measurements and rare earth element inversions. Journal of Geophysical Research: Solid Earth 97, 19683–19715.
Williams, H., Turner, S., Kelley, S., Harris, N., 2001. Age and composition of dikes in Southern Tibet: new constraints on the timing of east-west extension and its relationship to postcollisional volcanism. Geology 29, 339–342.
Wilson, D.S., Jamieson, S.S.R., Barrett, P.J., Leitchenkov, G., Gohl, K., Larter, R.D., 2012. Antarctic topography at the Eocene–Oligocene boundary. Palaeogeogr. Palaeoclimatol. Palaeoecol. 335–336, 24–34.
Wold, C., 1995. Palaeobathymetric reconstruction on a gridded database: the northern North Atlantic and southern Greenland-Iceland-Norwegian Sea. Geol. Soc. Lond., Spec. Publ. 90, 271–302.
Woodruff, F., Savin, S.M., 1989. Miocene deepwater oceanography. Paleoceanography 4, 87–140.
Wright, J.D., Miller, K.G., 1996. Control of North Atlantic deep water circulation by the Greenland-Scotland Ridge. Paleoceanography 11, 157–170.
Wright, J.D., Miller, K.G., Fairbanks, R.G., 1992. Early and Middle Miocene stable isotopes: implications for deepwater circulation and climate. Paleoceanography 7, 357–389.
Xu, X., Lithgow-Bertelloni, C., Conrad, C.P., 2006. Global reconstructions of Cenozoic seafloor ages: implications for bathymetry and sea level. Earth Planet. Sci. Lett. 243, 552–564.

Yang, S., Galbraith, E., Palter, J., 2014. Coupled climate impacts of the Drake Passage and the Panama Seaway. Clim. Dyn. 43, 37–52.
Zachos, J., Pagani, M., Sloan, L., Thomas, E., Billups, K., 2001. Trends, rhythms, and aberrations in global climate 65 Ma to present. Science 292, 686–693.
Zachos, J.C., Dickens, G.R., Zeebe, R.E., 2008. An early Cenozoic perspective on greenhouse warming and carbon-cycle dynamics. Nature 451, 279–283.
Zhang, Z., Nisancioglu, K., Flatøy, F., Bentsen, M., Bethke, I., Wang, H., 2011. Tropical seaways played a more important role than high latitude seaways in Cenozoic cooling. Clim. Past 7, 801–813.

E.O. Straume is a PhD research fellow at the Centre for Earth Evolution and Dynamics (CEED), at the Department of Geosciences, University of Oslo (2016–2020). He completed a MSc in geophysics/geodynamics from the University of Oslo in 2016. He is working within the field of paleoenvironment reconstructions and paleoclimate modelling. His main research interest is the evolution of oceanic basins and how changes in paleobathymetry have influenced ocean circulation and climate on geological timescales.

C. Gaina (PhD 1999, University of Sydney, Australia) is Professor of Marine Geophysics at University of Oslo, Norway and leads the Norwegian Centre of Excellence CEED (Centre for Earth Evolution and Dynamics) hosted by the Department of Geosciences, University of Oslo. She studies the evolution of the global oceanic regions as a key component of our dynamic planet by using a variety of geophysical and geological constraints. In particular, she is interested in revealing the role of tectonic processes to long-term climate evolution. For the last couple of years Carmen studied the complex evolution of the margins and oceanic basins in the North Atlantic, Arctic, and Indian oceans, and in the Circum-Antarctic and South East Asia regions. Furthermore, she led or participated in large geophysical dataset compilations and interpretations within several international projects (Northeast Atlantic Tectonics and Circum Arctic Mapping Programme). As a recognition for her national and international scientific work, she was elected a Member of the Norwegian Academy of Science and Letters, and a Member of the Academia Europea.

S. Medvedev has a MSc in continuum mechanics from Moscow State University (Russia) and PhD in tectonics from Uppsala University (Sweden). After post-docs in Canada and Germany, he is now researcher in Oslo University (Physics of Geological Processes and now Centre of Earth Evolution and Dynamics). His main interest is in theory of numerical methods in geodynamics and relation between surface processes and lithospheric deformations.

K.H. Nisancioglu received his degree in climate dynamics from MIT in 2004 and is currently Professor at the Department of Earth Science, University of Bergen, and Professor II at the Department of Geosciences and the Center for Earth Evolution and Dynamics, University of Oslo, Norway. Prof. Nisancioglu's research and teaching is focused on the understanding the dynamics of past, present and future climate changes, with particular attention to the Arctic. His recent work as PI of the ERC project ice2ice, the first EU funded Synergy project in the Nordic countries, has been centred around understanding abrupt climate changes in the Arctic and how changes in sea ice impact the dynamics of the Greenland ice sheet.